Oscillatory magnetic coupling between metallic multilayers across superconducting spacers

1995 J. Phys.: Condens. Matter 7 5239

(http://iopscience.iop.org/0953-8984/7/27/010)

J. Phys.: Condens. Matter 7 (1995) 5239–5269. Printed in the UK

Oscillatory magnetic coupling between metallic multilayers across superconducting spacers

Ondřej Šipr†‡ and Balázs L Györffy†

† H H Wills Physics Laboratory, University of Bristol, Tyndall Avenue, Bristol BS8 1TL, UK
‡ Institute of Physics of the Czech Academy of Science, Cukrovarnická 10, 162 53 Praha 6, Czech Republic

Received 2 March 1995, in final form 5 May 1995

Abstract. In order to investigate magnetic coupling between metallic layers across superconducting spacers, we study a simple inhomogeneous free-electron model with exchange-split bands in the magnetic region and pairing interaction in the superconducting layers. We solve numerically the corresponding Bogoliubov–de Gennes equations for spin-dependent potentials for a one-dimensional geometry and find strong evidence that, while the magnetic coupling strength will oscillate as a function of the spacer layer thickness L, it is strongly damped. This damping can be described by purely exponential form $\exp(-L/D)$, where the damping length D is of the order of the coherence length ξ_0 of the superconductor. We discuss, briefly, the physical circumstances where such a cut-off of the oscillatory magnetic coupling may be observed.

1. Introduction

Metallic multilayers are hosts to a number of novel magnetic phenomena, such as perpendicular magnetic anisotropy, giant magnetoresistance and oscillatory magnetic coupling across non-magnetic spacers to mention but a few (see reviews of Mathon (1991) and Bruno and Györffy (1994) and references therein). In this paper, we wish to contribute to the understanding of the last one of these by investigating how the coupling is modified if the spacer becomes superconducting.

To be specific, let us consider two semi-infinite 'host' magnetic metals separated by a non-magnetic spacer of a thickness L, as depicted schematically in figure 1. Well below the Curie temperature of the host metals, their magnetizations M_1 and M_2 are temperature independent and their magnetic interaction energy δE_{12} is found to be of the form

$$\delta E_{12} = J(L) M_1 \cdot M_2 + \dots$$

where, to simplify matters, we have neglected higher-order corrections. Central to our concern is the, by now well established, experimental fact that the exchange coupling strength $J(L)$ is an oscillatory function of L (Heinrich *et al* 1990, Parkin *et al* 1990, Parkin 1991). In general, more than one period is observed and these are thought to be related to the extremal wave vectors connecting opposite sides of the Fermi surface of the spacer material in the direction of the layer growth (Edwards *et al* 1991, Bruno and Chappert 1991). Evidently, the problem is of such interest because the observed oscillations are so directly related to this most fundamental feature of the metallic state.

Clearly, a way to test the above conjecture is to perform experiments in which the Fermi surface changes and to observe the corresponding changes in the coupling. For example,

0953-8984/95/275239+31$19.50

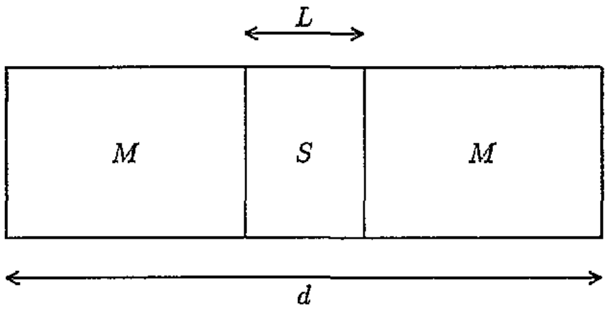

Figure 1. Schematic cross-section of the trilayer system investigated through this paper. The two host metals ('M') are generally magnetic (although we consider them for the sake of simplicity non-magnetic in some applications); the spacer metal ('S') between them is non-magnetic and may be superconducting. The total 'length' of the sandwich system d is much larger than the thickness of the spacer L, $d \gg L$, so that the chemical potential μ of the system does not change if L varies.

if the spacer metal is a superconductor, on lowering the temperature below its transition temperature T_c^S the above mechanism of magnetic coupling should be seriously disrupted. In order to stimulate experimental interest in this problem, we have worked out the main consequences of the existence of a superconducting gap on the oscillations of the magnetic coupling $J(L)$.

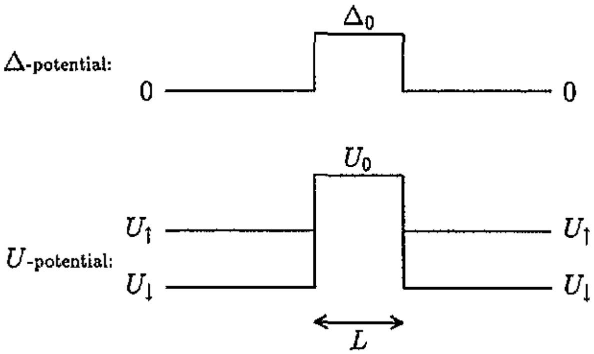

Figure 2. Schematic depiction of the normal U potential and of the pairing Δ potential inside the host and inside the spacer we use to model our trilayer system.

The basic jellium model we study (see figure 2) comprises two, semi-infinite magnetic metals separated by a superconductor. The magnets are defined by constant potentials $U_\uparrow$ and $U_\downarrow$ 'seen' by the $\uparrow$ and $\downarrow$ spin electrons, respectively. The superconductor is completely specified by the constant potential U_0 in the spacer layer and by the pairing potential $\Delta(\boldsymbol{r})$, which we consider to be uniform as well, $\Delta(\boldsymbol{r}) = \Delta_0$. We treat the spacer as an 'impurity', i.e. we assume that the host is connected to an infinite electron reservoir (in real terms, this means that we require $d \gg L$). Hence, the chemical potential μ is independent of L.

The approximation which sets the normal potential $U(x)$ to a constant is one which is adequate for investigating the nature of Friedel oscillations and oscillatory coupling phenomena (Bruno and Györffy 1993). Approximating the pairing potential $\Delta(x)$ by a constant is a more subtle matter. From the fundamental point of view, determining the pairing potential $\Delta(x)$ requires a self-consistency procedure by its very nature. In fact, assuming that $\Delta(x)$ is a constant we violate the gap equation. Nevertheless, the constant-gap approximation proved to work quite well in problems connected with superconducting layers (Plehn *et al* 1994). As we focus only on the essential features of the phenomena and do not attempt to simulate any particular material, we feel that the constant-gap approximation does not affect our conclusions significantly.

We are concerned with both a one- and a three-dimensional version of this model. In the former, the Y–Z dimensions transverse to the layer interfaces are neglected and in the latter it is assumed that all potentials are constant in both the Y and the Z directions.

To anticipate the consequences of the above model we note that an impurity in a superconductor induces an oscillatory distortion of the charge. As was shown by Fetter (1965), the functional form of these distortions is the same as that of the much studied Friedel oscillations in normal metals but with an exponential cut-off $\sim\exp(-r/D_0)$, where r is the radial distance from the impurity site and the damping length D_0 is of the order of the Bardeen–Cooper–Schrieffer (BCS) superconducting coherence length ξ_0. As is well known, charge or magnetization oscillations about each point defect in a two-impurity system give rise to a coupling energy between them that itself is an oscillatory function of their separation. Generically, such coupling is often referred to as RKKY (Ruderman, Kittel, Kasuya and Yosida) interaction. As was argued by Bruno and Györffy (1993), the oscillatory magnetic coupling $J(L)$ in metallic multilayers may be regarded as the planar defect version of the above RKKY interaction. From these arguments it follows that an exponential cut-off of the Friedel oscillations in a superconductor may translate into a similar cut-off of $J(L)$. The first purpose of this paper is to find out whether this indeed is the case.

Unfortunately, a thin-film superconductor will remain superconducting only if its thickness L is above a certain critical size $L_c \sim \xi_0$, and L_c may be too large for an observable magnetic coupling to arise. Moreover, the exchange interaction between the magnetic regions and the superconducting spacer may suppress the superconductivity. Our second purpose is to investigate the circumstances where the exponential damping of the magnetic coupling $J(L)$ might be, nevertheless, observable.

The scope of this paper is as follows. In section 2, a brief summary of the theoretical framework employed is presented. Particular emphasis is laid on handling the spin-dependent normal potential and on the way the physically relevant quantities (such as the electron density $n(\boldsymbol{r})$, the pairing amplitude $\chi(\boldsymbol{r})$ and the grand canonical potential of our system Ω_{tot}) are obtained. A few more technically oriented details related to this section are elaborated in appendices A and B. Friedel-like oscillations of the electron density and of the pairing amplitude for planar defects are investigated in section 3 both for a one-dimensional and for a three-dimensional geometry. The conjectured exponential decay of the oscillatory magnetic coupling across superconducting spacers is tested for a one-dimensional geometry in section 4 within the framework of interface–interface forces. Appendices C and D are related to that section. Finally, in section 5, we briefly address the question of whether the suppression of the magnetic coupling by superconductivity might be observed experimentally and in what sort of system such an effect should be most pronounced.

2. A summary of the theoretical framework

For clarity, in this section, we want to recall the basic equations we have relied upon and give a brief outline of the methods we employed in solving them yielding the results presented in the following sections.

2.1. Bogoliubov–de Gennes equations for a system with a spin-dependent normal potential

Bogoliubov–de Gennes (BdG) equations proved to provide a very efficient fully microscopic framework for investigating inhomogeneous superconductors. In a spin-independent form, they were applied to studies of superconductor–normal metal slab systems in numerous cases (see e.g. Entin-Wohlman and Bar-Sagi 1978, Zaitlin 1982, Tanaka *et al* 1991). As the use of the spin-dependent BdG equations is not so widespread and in order to make easier the comparison with the spin-dependent equations presented elsewhere (de Gennes 1966, Jin and Ketterson 1989), we give a brief outline of the derivation in appendix A. Here we quote just the final form of BdG equations for an s wave pairing and a spin-dependent normal potential,

$$\begin{aligned} &[H_e(\boldsymbol{r}) + U_\alpha(\boldsymbol{r})]\, u_{n\alpha}(\boldsymbol{r}) + \Delta_{\alpha,-\alpha}(\boldsymbol{r})\, v_{n,-\alpha}(\boldsymbol{r}) = E_{n\alpha}\, u_{n\alpha}(\boldsymbol{r}) \\ &-[H_e^*(\boldsymbol{r}) + U_{-\alpha}(\boldsymbol{r})] v_{n,-\alpha}(\boldsymbol{r}) + \Delta^+_{-\alpha,\alpha}(\boldsymbol{r})\, u_{n\alpha}(\boldsymbol{r}) = E_{n\alpha}\, v_{n,-\alpha}(\boldsymbol{r}) \end{aligned} \tag{1}$$

where $\alpha = \uparrow$ or $\alpha = \downarrow$, $u_{n\alpha}(\mathrm{r})$ and $v_{n,\alpha}(\boldsymbol{r})$ are spin-dependent probability amplitudes that the quasiparticle at $\boldsymbol{r}$ is a particle or a hole, respectively. The Hamiltonian H_e, the normal spin-dependent potential $U_\alpha(\boldsymbol{r})$ and the pairing potential $\Delta_{\alpha,-\alpha}(\boldsymbol{r})$ are defined in appendix A. In what follows we shall refer to the normal potential $U_\alpha(\mathrm{r})$ as the 'U potential' and to the pairing potential $\Delta_{\alpha,-\alpha}(\boldsymbol{r})$ as the 'Δ potential' for brevity.

Equations (1) reduce to the standard spin-independent form of BdG equations (de Gennes 1966) if the identifications $\Delta_{\uparrow\downarrow}(\boldsymbol{r}) = \Delta(\boldsymbol{r})$, $u_\uparrow(\boldsymbol{r}) = u(\boldsymbol{r})$, $u_\downarrow(\boldsymbol{r}) = u(\boldsymbol{r})$, $v_\downarrow(\boldsymbol{r}) = v(\boldsymbol{r})$ and $v_\uparrow(\boldsymbol{r}) = -v(\boldsymbol{r})$ are made.

The density of spin-up and spin-down electrons at zero temperature is given by

$$n_\alpha(\boldsymbol{r}) = \sum_n |v_{n\alpha}(\boldsymbol{r})|^2 \tag{2}$$

and the pairing amplitude $\chi_{\alpha\beta}(\boldsymbol{r})$ (see appendix A for more clarification) can be expressed as follows:

$$\chi_{\alpha\beta}(\boldsymbol{r}) = \sum_n u_{n\alpha}(\boldsymbol{r})\, v^*_{n\beta}(\boldsymbol{r})\, \delta_{\alpha,-\beta}. \tag{3}$$

The total grand canonical potential of a superconductor at $T = 0$, $\Omega_{tot} = \langle H_{eff}\rangle$ (cf. the definitions (A1) and (A2)), can be shown to be

$$\Omega_{tot} = \sum_\alpha \sum_n (-E_{n\alpha}) \int \mathrm{d}^3 r\, |v_{n,-\alpha}(\boldsymbol{r})|^2. \tag{4}$$

Through this paper, we take the pairing potential $\Delta(\mathbf{r})$ to be given, i.e. no gap equation is solved.

For a computational convenience, it is useful to transform the two pairs of equations given in (1) into a single pair by allowing E to be negative. A straightforward manipulation shows that to find a full set of solutions of the system in (1) is equivalent to solving two coupled equations (we omit the subscript n for brevity)

$$\begin{aligned} &[H_e(\boldsymbol{r}) + U_\uparrow(\boldsymbol{r})]\, u(\boldsymbol{r}) + \Delta(\boldsymbol{r})\, v(\boldsymbol{r}) = E\, u(\boldsymbol{r}) \\ &-[H_e^*(\boldsymbol{r}) + U_\downarrow(\boldsymbol{r})]\, v(\boldsymbol{r}) + \Delta^*(\boldsymbol{r})\, u(\boldsymbol{r}) = E\, v(\boldsymbol{r}) \end{aligned} \tag{5}$$

for both positive and negative energies and then identifying for positive-energy solutions ($E > 0$)

$$\begin{aligned} &u_\uparrow(\boldsymbol{r}) = u(\boldsymbol{r}) \\ &v_\downarrow(\boldsymbol{r}) = v(\boldsymbol{r}) \\ &E_\uparrow = E \end{aligned} \tag{6}$$

and for negative-energy solutions ($E < 0$)

$$
\begin{aligned}
u_{\downarrow}(\boldsymbol{r}) &= v^*(\boldsymbol{r}) \\
v_{\uparrow}(\boldsymbol{r}) &= u^*(\boldsymbol{r}) \\
E_{\downarrow} &= -E.
\end{aligned}
\tag{7}
$$

This approach has been adopted throughout this paper.

Surprisingly, solving the BdG equations numerically for a three-dimensional inhomogeneous superconductor is not a trivial task even for the very simple model outlined above. To circumvent the central difficulty, arising from a subtle interplay between short and large length scales, k_F^{-1} and ξ_0, respectively, a very successful 'semiclassical' or 'Andreev' or 'WKB' approximation was introduced by Andreev (1964) and Bardeen *et al* (1969). A thorough discussion of various formulations of the semiclassical approximation can be found e.g. in Kobes and Whitehead (1987), Ashida *et al* (1989) or in Clinton (1992). Most microscopic calculations for inhomogeneous problems are tackled in this way. However, as the semiclassical approximation focuses only on variations on the scale of ξ_0 and ignores variations on the scale of k_F^{-1}, it cannot be relied on when investigating problems related to Friedel oscillations. It may be useful to note that whenever the semiclassical approximation was employed in the past, the main concern was a pairing potential $\Delta(x)$ varying slowly on the spatial scale k_F^{-1} (Kieselman 1987, Ashida *et al* 1989, Tanaka *et al* 1991, Hara *et al* 1993). On the other hand, when similar systems possessing planar symmetry were investigated within an exact theory, rapid Friedel-like oscillations were obtained (Tanaka and Tsukada 1989, Stojković and Valls 1994).

The final remark of this section concerns the units: to make the results more easy to read, we measure energy throughout this paper in units of Fermi energy E_F and distances in units of reciprocal Fermi wavevector $k_F = \sqrt{E_F}$. The only exception is section 5 where Rydberg atomic units are used to simplify the comparison of our numerical values with possible experimental data (note that all the equations and the results keep their form if E_F is substituted by any other 'reference' energy E_R).

2.2. *Solution of BdG equations for a plane geometry*

In order to solve system (5) for a plane geometry, i.e. in the case where the potentials $U_{\downarrow}(\boldsymbol{r})$, $U_{\uparrow}(\boldsymbol{r})$ and $\Delta(\boldsymbol{r})$ are non-uniform in the X direction only, we separate the variables x, y and z by setting

$$
\begin{aligned}
u(\boldsymbol{r}) &= u(x)\,\frac{1}{2\pi}\;\mathrm{e}^{\mathrm{i}\,(k_y y + k_z z)} \\
v(\boldsymbol{r}) &= v(x)\,\frac{1}{2\pi}\;\mathrm{e}^{\mathrm{i}\,(k_y y + k_z z)}.
\end{aligned}
$$

The 'one-dimensional' wave-functions $u(x)$, $v(x)$ then satisfy the equations

$$
\begin{aligned}
&-\frac{\mathrm{d}^2}{\mathrm{d}x^2}\,u(x) + [U_{\uparrow}(x) - \mu_t - E]\,u(x) + \Delta(x)\,v(x) = 0 \\
&\frac{\mathrm{d}^2}{\mathrm{d}x^2}\,v(x) + [-U_{\uparrow}(x) + \mu_t - E]\,v(x) + \Delta^*(x)\,u(x) = 0
\end{aligned}
\tag{8}
$$

where a new variable $\mu_t \equiv \mu - \left(k_y^2 + k_z^2\right)$ has been introduced (note that always $\mu_t < \mu$).

The solutions of a one-dimensional BdG equation (8) for a piece-wise constant potential are constructed in such a way that, first a fundamental system of solutions in the host and in the spacer regions are found, and then they are matched across the interface so that the

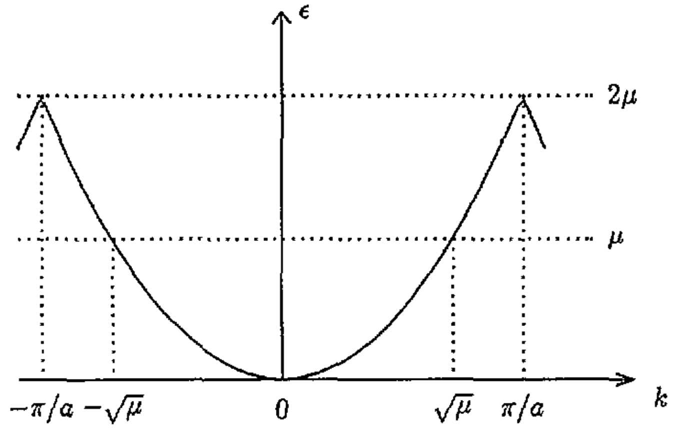

Figure 3. Intuitive interpretation of our model in terms of a half-filled parabolic band. The vertical axis shows single-particle energy ϵ, the horizontal axis shows the reciprocal lattice 'k vector'. The quasiparticle energy of the states below the chemical potential (i.e. holes) is $E = \mu - \epsilon$; the quasiparticle energy of the states above the chemical potential (i.e. particles) is $E = \mu + \epsilon$. The lattice constant of our auxiliary periodic system is a; the width of the half-filled band is 2μ.

wave-functions $u(x)$, $v(x)$ together with their first derivatives remain continuous. In the host region ($|x| > L/2$), the solutions can be written in terms of functions

$$\begin{pmatrix} u_h \\ v_h \end{pmatrix} e^{\pm i\gamma_1 x} \qquad \begin{pmatrix} v_h \\ u_h \end{pmatrix} e^{\pm i\gamma_2 x} \tag{9}$$

where (note that E may be both positive and negative in our formalism)

$$u_h = E + |E| \qquad v_h = E - |E|$$

and the frequencies are (see figure 2 for the notation)

$$\gamma_1 = \sqrt{\mu_t - U_\uparrow + |E|} \tag{10}$$

$$\gamma_2 = \sqrt{\mu_t - U_\downarrow - |E|} \tag{11}$$

for $E > 0$ (see equation (6)) or

$$\gamma_1 = \sqrt{\mu_t - U_\downarrow + |E|} \tag{12}$$

$$\gamma_2 = \sqrt{\mu_t - U_\uparrow - |E|} \tag{13}$$

for $E > 0$ (see equation (7)). In the spacer region ($|x| < L/2$) the solutions are

$$\begin{pmatrix} u_s \\ v_s \end{pmatrix} e^{\pm i\omega_1 x} \qquad \begin{pmatrix} v_s \\ u_s \end{pmatrix} e^{\pm i\omega_2 x} \tag{14}$$

where

$$u_s = E + \Delta_0 + \sqrt{E^2 - \Delta_0^2}$$

$$v_s = E + \Delta_0 - \sqrt{E^2 - \Delta_0^2}$$

and the frequencies are

$$\omega_1 = \sqrt{\mu_t - U_0 + \sqrt{E^2 - \Delta_0^2}} \tag{15}$$

$$\omega_2 = \sqrt{\mu_t - U_0 - \sqrt{E^2 - \Delta_0^2}} \tag{16}$$

for both $E > 0$ and $E < 0$.

For imaginary frequencies γ_1, γ_2, only those exponentials in (9) which do not destroy the normalizability of the solution are kept.

In order to calculate the electron density etc, we have to sum over a complete set of orthonormal solutions (see equations (2)–(4)). In the case of symmetrical U and Δ potentials, normalizable solutions of equation (8) for a given E and μ_t can be chosen so that they are either even ($\ell = 0$) or odd ($\ell = 1$). Moreover, for certain values of E and μ_t, there exist two linearly independent solutions for each ℓ—we distinguish them by the index j (in a non-superconducting case, this corresponds to the fact that a quasiparticle with an excitation energy below the chemical potential can be either a particle or a hole).

Solutions corresponding to different E, μ_t or ℓ are already orthogonal by their construction. Solutions corresponding to identical E, μ_t and ℓ but different j do not come out orthogonal naturally and may need explicit orthogonalization. If the 'scalar product' of two solutions $u_{E,1}(x), v_{E,1}(x)$ and $u_{E,2}(x), v_{E,2}(x)$ (we have omitted other indexes for simplicity) is

$$\int \mathrm{d}x\ [u^*_{E,1}(x)u_{E',2}(x) + v^*_{E,1}(x)v_{E',2}(x)] = F(E)\,\delta(E - E') \tag{17}$$

where the function $F(E)$ is not identically zero, a new set of orthogonal solutions can be generated by a sort of Gramm–Schmidt orthogonalization procedure so that the new couple of solutions already satisfies equation (17) with $F(E) \equiv 0$. An example of such a procedure is given e.g. in Kobes and Whitehead (1987).

Our choice of the wave-functions is made in such a way that if two linearly independent solutions exist for given E, μ_t and ℓ, the first one ($j = 1$) contains only functions (14) with the frequency ω_1 in the spacer region. The second solution ($j = 2$) is chosen to be orthogonal to the first one and although it contains functions of both frequencies in the spacer region, functions with the frequency ω_2 are usually present with a 'bigger weight'. In short, the $j = 1$ solution corresponds mainly to a particle while the $j = 2$ solution corresponds mainly to a hole.

Writing the wave-function indexes explicitly, the sum $\sum_n$ of equations (2)–(4) becomes

$$\begin{aligned}\sum_n f_n \ \to\ & \int \mathrm{d}E \int \mathrm{d}k_y \int \mathrm{d}k_z \sum_\ell \sum_j f_{E,\mu-(k_y^2+k_z^2),\ell,j} \\ &= \pi \int \mathrm{d}E \int \mathrm{d}\mu_t \sum_\ell \sum_j f_{E,\mu_t,\ell,j}\end{aligned} \tag{18}$$

where the function $f_{E,\mu_t,\ell,j}$ stands collectively for any of the terms summed upon in (2)–(4).

The matching conditions give rise to a set of four linear algebraic equations. Although explicit analytical formulas for the solutions of these equations can be written, we solve them rather numerically as this provides actually more accurate values in the end (due to a better numerical stability). As we intend to integrate numerically equations (2)–(4) and to look for oscillations which may not exceed 10^{-6} of the underlying value, the accuracy is of a crucial importance to us.

The last 'technical' remark concerns the upper bound of the E integral in (18): if no cut-off is introduced the integrals (3), (4) diverge (see appendix B and the discussion therein). In order to prevent this, in all our calculations involving equations (2)–(4), we cut the energy integrals at the same limit E_C. We choose $E_C = 1.10\,E_F$ in order to take account of the possible effect of holelike quasiparticles with energies a bit larger than the chemical potential $\mu = 1.0\,E_F$. We have tested that the conclusions drawn from our numerical results do not depend on the particular choice of E_C, provided that E_C is not too low (say not less than $\sim 1.05\, E_F$ for all the systems investigated throughout this paper).

It is possible to get a physically intuitive interpretation of this cut-off, if one assumes that in our model we are dealing with a 'half-filled jellium band' (see figure 3), hence cutting off the states outside it. If we think of our half-filled parabolic band as being created by a lattice with a lattice constant a, then from the dispersion relation at the Brillouin zone boundary

$$2\,\mu = \left(\frac{1}{2}\,\frac{2\pi}{a}\right)^2$$

we get that our lattice constant would be $a = 2.221/\sqrt{\mu}$. Clearly, this relation establishes a connection between measuring the lengths in reciprocal Fermi wave-vectors $k_F^{-1} = 1/\sqrt{\mu}$ and in atomic layer distances a.

3. Friedel oscillations for planar defects

As has been discovered by Friedel, the electron density disturbed by the presence of an impurity acquires its asymptotic ('host') value in an oscillatory rather than a monotonic way. The period of these oscillations is closely related to the Fermi surface. In a normal state ($\Delta(x) = 0$), the 'excess electron density'

$$\delta n(\boldsymbol{r}) = n(\boldsymbol{r}) - n_0 \tag{19}$$

around a spherical impurity (n_0 is the electron density of an unperturbed homogeneous host) can be written in the asymptotic ($r \to \infty$) region as

$$\delta n(\boldsymbol{r}) \;\sim\; \frac{1}{r^3} \sum_{\ell=0}^{\infty} (-1)^\ell\,(2\ell+1)\,\sin[\delta_\ell(E_F)]\,\cos[2k_F r + \delta_\ell(E_F)] \tag{20}$$

where the phase shifts $\delta_\ell(E)$ fully describe the influence of the impurity on the electron wave-function (Ziman 1964).

Fetter (1965) investigated the effect of a spherical impurity on of an otherwise homogeneous infinite superconductor with a pairing potential $\Delta(\boldsymbol{r}) = \Delta_0$. He observed Friedel-like oscillations both in the electron density and in the pairing amplitude. Particularly, in the case of a hard-sphere U potential impurity (i.e. $U_0 \to \infty$ in our notation), he found for $T \approx 0$ the asymptotic form of the electron density

$$\delta n(\boldsymbol{r}) \;\sim\; \frac{1}{r^3} \sum_{\ell=0}^{\infty} (-1)^\ell\,(2\ell+1)\,\sin[\delta_\ell(E_F)] \times \cos[2k_F r + \delta_\ell(E_F)]\,\left(1+\frac{r}{D_0}\right)\exp\left(-\frac{r}{D_0}\right) \tag{21}$$

and of the pairing amplitude

$$\delta\chi(\boldsymbol{r}) \sim \frac{1}{r^2} \sum_{\ell=0}^{\infty} (-1)^\ell\,(2\ell+1)\,\sin[\delta_\ell(E_F)]\,\left\{\frac{1}{k_F r}\cos[\delta_\ell(E_F)] + 2\sin[2k_F r + \delta_\ell(E_F)]\left[\exp\left(-\frac{r}{D_0}\right) + E_1\left(\frac{r}{D_0}\right)\right]\right\}. \tag{22}$$

In both of the above expressions, the damping factor D_0 is given by

$$D_0 = \tfrac{1}{2}\pi\xi_0 \tag{23}$$

where ξ_0 is the usual BCS coherence length, namely $\xi_0 = \hbar v_F/(\pi\Delta_0)$ with v_F standing for the Fermi velocity. Moreover, the exponential integral $E_1(x)$ is given by

$$E_1(x) = \int_x^\infty \mathrm{d}t\, \frac{1}{t}\, \mathrm{e}^{-t}$$

and the 'excess pairing amplitude' $\delta\chi(r)$ is defined analogously to (19), viz.

$$\delta\chi(r) = \chi(r) - \chi_0 \tag{24}$$

where χ_0 clearly is the uniform pairing amplitude of the host in the absence of the impurity.

The equations (21) and (22) show that the period of the oscillations remains the same as in a non-superconducting case, while the power law decay of these oscillations (cf. equation (20)) is modified basically by an exponentially decaying factor. The precise asymptotic form of this damping can be found if one keeps only lowest-order terms in $(1/r)$ in equations (21) and (22) and considers that asymptotically

$$E_1(x) \to \frac{1}{x}\mathrm{e}^{-x}.$$

Then, one finds for $T \approx 0$ that, in case of a hard-sphere spherical impurity, both the electron density and the pairing amplitude oscillations decay as

$$\sim \frac{1}{r^2} \exp\left(-\frac{r}{D_0}\right). \tag{25}$$

By contrast, for $T \approx T_c^S$, the power law parts of the asymptotic decay forms are r^{-3} and r^{-2} for the electron density $n(r)$ and for the pairing amplitude $\chi(r)$, respectively (Fetter 1965).

A one-dimensional system (and, consequently, a three-dimensional system with a planar symmetry as well) can be formally treated on the same footing as spherically symmetric systems, provided that the angular momentum quantum number ℓ is substituted with the parity taking $\ell = 0$ for even wavefunctions and $\ell = 1$ for odd ones (Butler 1976). To investigate a non-superconducting system consisting of a plane (slablike) impurity in an otherwise homogeneous host, we applied procedures very similar to those employed by Bruno and Győrffy (1993). For a one-dimensional geometry and $T = 0$, the asymptotic form of the electron density oscillations $\delta n(x)$ is

$$\delta n(x) \sim \frac{1}{x} \sum_{\ell=0}^{1} (-1)^\ell \sin[\delta_\ell(E_F)] \cos[2k_F x + \delta_\ell(E_F)] \tag{26}$$

while for a proper three-dimensional case we get

$$\delta n(x) \sim \frac{1}{x^2} \sum_{\ell=0}^{1} (-1)^\ell \sin[\delta_\ell(E_F)] \sin[2k_F x + \delta_\ell(E_F)] \tag{27}$$

provided that one-dimensional phase shifts $\delta_\ell(E)$ are suitably defined.

Although the results of Fetter (1965) cannot be readily generalized to our situation, it is natural to expect that the basic trends accompanying the transition from a non-superconducting to a superconducting system are preserved. Hence, we conjecture that the power law asymptotic decay forms of the electron density and of the pairing amplitude are modified by superconductivity into an exponential damping of the form (cf. equations (21), (22) and (26), (27))

$$\sim \frac{1}{x^n} \exp(-\frac{x}{D})$$

with the damping length D being of order of the 'Fetter' damping length D_0 and the power n of order unity.

To investigate this problem further, we calculate, numerically, the electron density and the pairing amplitude for a model system containing a slablike impurity both in one and in three dimensions. A *non-superconducting* system containing such a defect in $U(x)$ is described by

$$\begin{array}{lll} U \text{ potential:} & U(x) = U_0 \text{ if } |x| < L/2 & U(x) = 0 \text{ if } |x| > L/2 \\ \Delta \text{ potential:} & \Delta(x) = 0 \;\forall x. & \end{array} \tag{28}$$

For a *superconducting* system with a slablike defect in $U(x)$ we have

$$\begin{array}{lll} U \text{ potential:} & U(x) = U_0 \text{ if } |x| < L/2 & U(x) = 0 \text{ if } |x| > L/2 \\ \Delta \text{ potential:} & \Delta(x) = \Delta_0 \;\forall x. & \end{array} \tag{29}$$

In three dimensions, we assume that the system is homogeneous both in Y and in Z directions.

Before our results are presented, a few technical remarks are in order. The electron density $n(x)$ and the pairing amplitude $\chi(x)$ are determined by equations (2), (3) and (18). The integration region in the (E, μ_t) plane is restricted in part by the conditions $E < E_C$ and $\mu_t < \mu$ (see text after equation (B2) in appendix B) and in part by the requirement that the wave-functions have to be normalizable. This later restriction can be expressed in conditions laid on the frequencies (10)–(13) of the solutions in the host region. Whenever γ_1 is real and γ_2 imaginary, there is just one normalizable independent solution to BdG equations (8). Whenever both γ_1 and γ_2 are real, there are two normalizable solutions.

Note that if (2)–(4) are to be integrated for a non-superconducting system (i.e. $\Delta(x) = 0$ everywhere), no double integration in (18) actually needs to be performed—it can be reduced to a single one by straightforward analytical manipulations (making use of the fact that if the two equations (8) can be decoupled, the solutions depend on E and on μ_t only through their combinations $\mu_t + E$ or $\mu_t - E$). However, if $\Delta(x) \neq 0$, this reduction cannot be made and a full two-dimensional integral has to be performed. This makes the numerical computation an order of magnitude more demanding in the CPU time.

In order to decrease the minimum density of the (E, μ_t)-mesh which is necessary for achieving the required accuracy, we found it convenient to slice the whole two-dimensional integration region not according to the E and μ_t variables but according to E and γ_i, where γ_i are the frequencies of the solutions (9) in the host region. In the region where only one linearly independent solution for each E, μ_t and ℓ exists (see text before equation (18)), our choice of the integration variables is (E, γ_1). In the region where there are two independent solutions for each E, μ_t and ℓ, the integration is done in (E, γ_1) variables when dealing with the first ($j = 1$) solution and in (E, γ_2) variables when dealing with the second ($j = 2$) one. Such a choice of integration variables means that, in case of a non-superconducting system, the integrands in (2) and (3) do not, for a fixed γ_2, depend on E at all.

3.1. Slablike impurity in one dimension

First, let us study the case of a U perturbation in one dimension. The general form of the potentials is presented in equations (28) and (29). The numerical values of the various parameters throughout this section are $U_0 = 0.20E_F$, $L = 20k_F^{-1}$ and $\mu = 1.0E_F$; the pairing potential is either $\Delta_0 = 0$ for a normal system or $\Delta_0 = 0.03E_F$ for a superconducting one. The exponential damping length is being expressed in terms of the Fetter damping length D_0 defined by (23). All our calculations are performed for a zero temperature, $T = 0$. We checked that both the excess electron density $\delta n(x)$ and the excess pairing amplitude $\delta\chi(x)$ are well converged with respect to the cut-off energy E_C (see end of section 2.2).

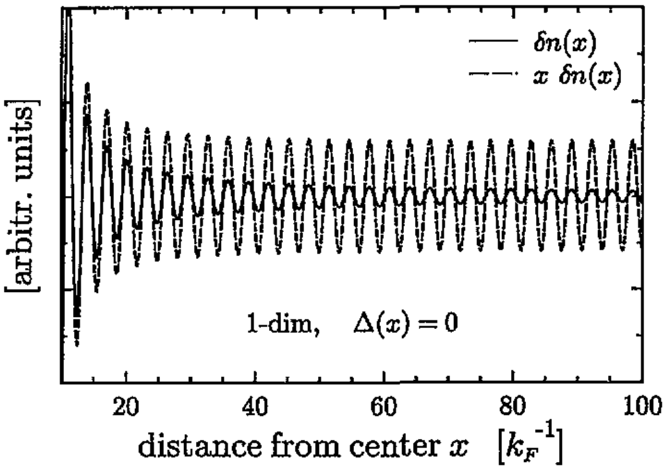

Figure 4. Analysis of the asymptotic behaviour of the electron density $n(x)$ as a response to a slablike U potential perturbation in a *non-superconducting* one-dimensional system. The excess electron density $\delta n(x) = n(x) - n_0$ together with the $x\,\delta n(x)$ curve are presented. The x-coordinate is measured from the centre of the impurity.

In order to test the way in which the oscillations decay, we plot the $\delta n(x)$ results together with the $\delta n(x)$ oscillations multiplied by the distance from the centre x, and in the superconducting case also by the exponentially varying factor $\exp(x/D)$. The analysis of the asymptotic behaviour of the excess electron density $\delta n(x)$ for a normal host is presented in figure 4. It can be seen readily that the envelope of the $x\,\delta n(x)$ curve approaches a straight line, in agreement with equation (26). Note that the 'asymptotic' region begins quite soon, around $x \approx 30\,k_F^{-1}$.

A more interesting case of an analogous superconducting system is analysed in figures 5 and 6. In figure 5, the $\delta n(x)$ oscillations are presented together with an $x\,\delta n(x)$ curve and an $x\exp(x/D)\delta n(x)$ curve. We see immediately that the decay of $\delta n(x)$ oscillations is quicker then just $1/x$. It can be observed also that if the damping length D is suitably chosen ($D = 1.3\,D_0$ in figure 5), the envelope of the $x\exp(x/D)\delta n(x)$ curve tends to a horizontal line asymptotically. This demonstrates that the electron density oscillations decay as

$$\delta n(x) \sim \frac{1}{x}\exp\left(-\frac{x}{D}\right) \tag{30}$$

in our one-dimensional model.

The oscillations in the pairing amplitude $\delta\chi(x)$ in a superconducting system are analysed in a similar way in figure 6. In this case, it was not possible to fit the $\delta\chi(x)$ decay to the asymptotic form given in equation (30). However, it can be described by a purely exponential decay, namely

$$\delta\chi(x) \sim \exp\left(-\frac{x}{D}\right) \tag{31}$$

provided that the damping length is set to $D = 0.9\,D_0$, as demonstrated in figure 6.

The frequency of the oscillations both in $\delta n(x)$ and in $\delta\chi(x)$ remains unaffected by the superconductivity and is $2k_F$ as in the normal state.

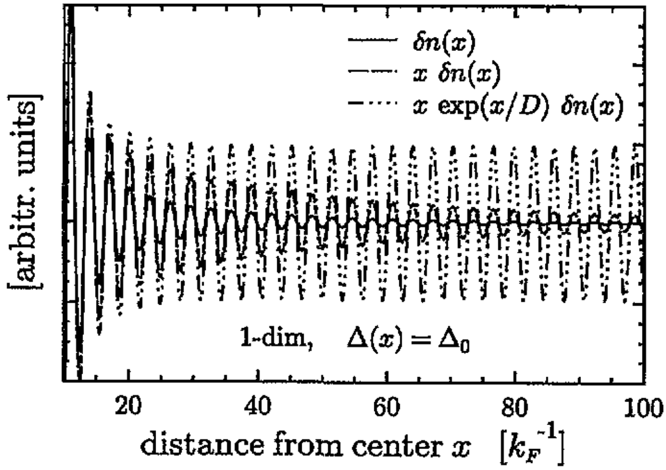

Figure 5. Analysis of the asymptotic behaviour of the electron density $\delta n(x)$ as a response to a slablike U potential perturbation in a *superconducting* one-dimensional system. The excess electron density $\delta n(x)$ together with the $x\,\delta n(x)$ and the $x\,\exp(x/D)\,\delta n(x)$ curves are presented. The exponential damping length is $D = 1.3\,D_0$, D_0 being the Fetter damping length (see text for details).

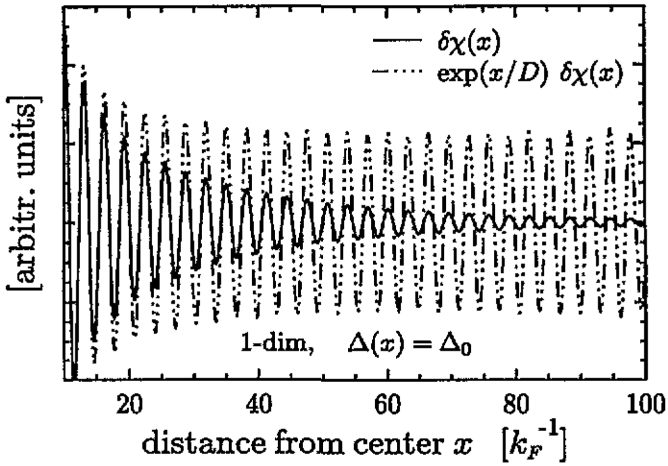

Figure 6. Analysis of the asymptotic behaviour of the pairing amplitude $\delta\chi(x)$ as a response to a slablike U potential perturbation in a *superconducting* one-dimensional system. The excess pairing amplitude $\delta\chi(x) = \chi(x) - \chi_0$ together with the $\exp(x/D)\,\delta\chi(x)$ curve are presented. The exponential damping length is $D = 0.9\,D_0$.

3.2. Slablike impurity in three dimensions

In this section, results for a proper three-dimensional system perturbed by a slablike impurity are presented. The form of the U and Δ potentials remains unchanged and is described by (28) and (29). The numerical values of the parameters U_0, L, μ and Δ_0 are the same as mentioned at the beginning of section 3.1.

The electron density oscillations induced by a slablike impurity in a normal system are described by equation (27). To enable an easier comparison with the superconducting case, the system was also investigated numerically. The results are summarized in figure 7. The

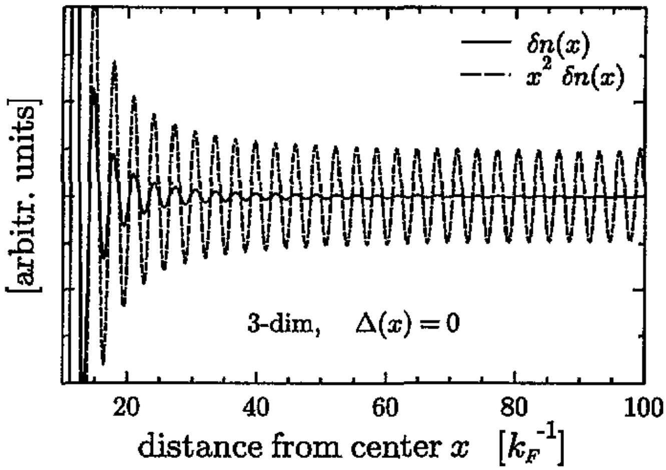

Figure 7. Analysis of the asymptotic behaviour of the electron density $n(x)$ as a response to a slablike U potential perturbation in a *non-superconducting* three-dimensional system. The excess electron density $\delta n(x)$ together with the $x^2\,\delta n(x)$ curve are presented. The x-coordinate is measured from the centre of the impurity.

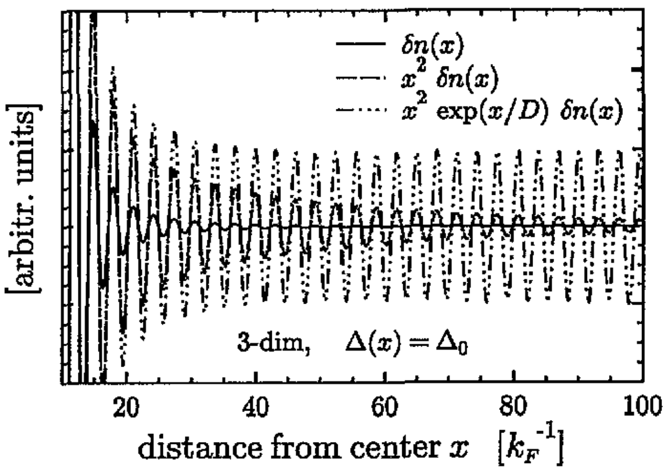

Figure 8. Analysis of the asymptotic behaviour of the electron density $\delta n(x)$ as a response to a slablike U potential perturbation in a *superconducting* three-dimensional system. The excess electron density $\delta n(x)$ together with the $x^2\,\delta n(x)$ and the $x^2\,\exp(x/D)\,\delta n(x)$ curves are presented. The exponential damping length is $D = 1.2\,D_0$.

'asymptotic region', where the x^{-2} decay is the dominant one, begins at $x \approx 40\,k_F^{-1}$.

A superconducting system is investigated in figures 8 and 9. The electron density oscillations $\delta n(x)$ decay as

$$\delta n(x) \sim \frac{1}{x^2}\exp\left(-\frac{x}{D}\right) \tag{32}$$

which is demonstrated in figure 8 (the decay length is $D = 1.2\,D_0$). The damping of the excess pairing amplitude $\delta\chi(x)$ oscillations is investigated in figure 9 and it can be described

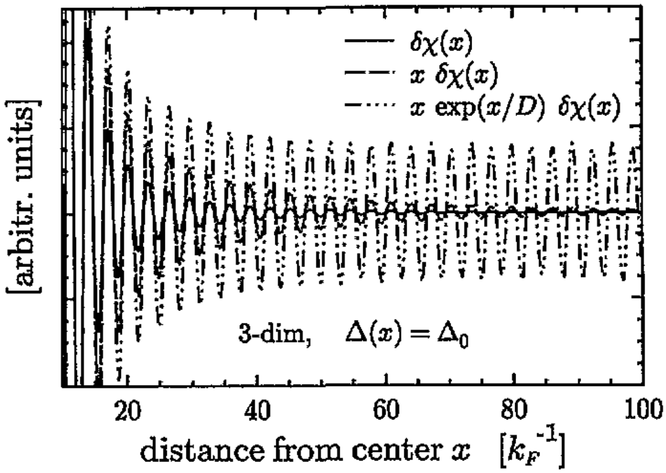

Figure 9. Analysis of the asymptotic behaviour of the pairing amplitude $\delta\chi(x)$ as a response to a slablike U potential perturbation in a *superconducting* three-dimensional system. The excess pairing amplitude $\delta\chi(x)$ together with the $x\,\delta\chi(x)$ and the $x\,\exp(x/D)\,\delta\chi(x)$ curves are presented. The exponential damping length is $D = 0.9\,D_0$.

by

$$\delta\chi(x) \sim \frac{1}{x}\exp\left(-\frac{x}{D}\right) \tag{33}$$

provided that the damping length is $D = 0.9\,D_0$.

It is not very easy to interpret our results. We have checked that the decay forms in equations (30)–(33) do not depend on the particular choice of numerical parameters used in our model (by performing a similar analysis for several other choices of U_0, L and Δ_0). The same is, however, not true for the decay lengths D, which, generally, vary both with Δ_0 and with the dimensionality: basically, the damping length D as measured in units of D_0 decreases with Δ_0 for $\delta n(x)$ oscillations and increases with with Δ_0 for $\delta\chi(x)$ oscillations in one dimension, while in three dimensions it rises with Δ_0 both for $\delta n(x)$ oscillations and for $\delta\chi(x)$ oscillations as well. The fact that the damping length D is not directly proportional to D_0 and hence to the superconducting coherence length ξ_0 is in contradiction with the findings of Fetter (1965) for a hard-sphere impurity. Similarly, in the system studied by Fetter, the exponential damping length was identical both for $\delta n(x)$ and for $\delta\chi(x)$ oscillations, which is not the case of the results presented here.

As expected, the frequency of the Friedel-like oscillations does not depend on Δ_0 or on the dimensionality. The power law part of the decay switches from x^{-2} to x^{-1} for the electron density and from x^{-1} to x^0 for the pairing amplitude oscillations when the dimensionality is changed from three to one. This is in agreement with the trend in non superconducting case, as described by equations (26)–(27).

Finally, we found for our system that the electron density $\delta n(x)$ decays more quickly than the pairing amplitude $\delta\chi(x)$ (compare (30) with (31) and (32) with (33)). In contrast, Fetter's results imply for $T = 0$ the same asymptotic form of decay both for $\delta n(x)$ and for $\delta\chi(x)$ (see equations (21), (22) and (25) in this paper or equation (110) in the original paper of Fetter (1965)).

To conclude this section, it is clear that some unexpected questions concerning the nature of Friedel-like oscillations in superconductors and their damping arise from our results, particularly as they disagree with the naive expectations based on Fetter (1965).

Although these are of interest in their own right they are not at the centre of our attention, which is the very fact of the exponential damping in this paper. Clearly, the evidence for an exponentially decreasing term $\sim\exp(-x/D)$ in the Friedel-like oscillations formulae nevertheless is compelling.

This suggests that the oscillatory coupling in magnetic multilayers will be exponentially damped if the spacer becomes superconducting. It is the purpose of the next section to verify this.

4. Interaction between two planar defects—oscillatory coupling

In the previous section, we studied Friedel oscillations *outside* a defect described by a potential barrier in $U(x)$. We have found that the oscillations in the electron density and in the pairing amplitude decay with increasing distance from the barrier, i.e. from the interface. Of course, in the same way as we have studied the oscillations inside the host it would be possible to study them inside the spacer. Clearly, if the thickness of the spacer decreases, the interaction of the two host/spacer interfaces should become more significant. This interface–interface interaction gives rise to an interesting physical phenomenon, viz. oscillatory coupling between the two host layers across the spacer. It is the magnetic version of this coupling that is attracting so much current attention (Bruno and Chapert 1991, Bruno and Györffy 1993).

In this section, we shall study this oscillatory coupling within framework of the interface–interface interactions. Following the line of the previous section, our main interest lies in comparing this coupling in the cases of a superconducting and a non-superconducting spacer. We will consider the case of a ferromagnetic host, since it is this case which is most accessible to experiments. Consequently, in the case of a non-superconducting spacer, we investigate the system described by (see figure 2)

$$\begin{aligned}
&U \text{ potential: } && U_\uparrow(x) = U_0 \text{ if } |x| < L/2 && U_\uparrow(x) = U_\uparrow \text{ if } |x| > L/2 \\
& && U_\downarrow(x) = U_0 \text{ if } |x| < L/2 && U_\downarrow(x) = U_\downarrow \text{ if } |x| > L/2 \\
&\Delta \text{ potential: } && \Delta(x) = 0 \ \forall x &&
\end{aligned} \tag{34}$$

and, for a superconducting spacer, by

$$\begin{aligned}
&U \text{ potential: } && U_\uparrow(x) = U_0 \text{ if } |x| < L/2 && U_\uparrow(x) = U_\uparrow \text{ if } |x| > L/2 \\
& && U_\downarrow(x) = U_0 \text{ if } |x| < L/2 && U_\downarrow(x) = U_\downarrow \text{ if } |x| > L/2 \\
&\Delta \text{ potential: } && \Delta(x) = \Delta_0(L) \text{ if } |x| < L/2 && \Delta(x) = 0 \text{ if } |x| > L/2.
\end{aligned} \tag{35}$$

For the actual calculations we have used the following parameter values: $U_0 = 0.20\,E_F$, $U_\uparrow = 0.10\,E_F$, $U_\downarrow = 0.00\,E_F$ and $\mu = 1.0\,E_F$. The spacer thickness L is now a variable and so is, in general, the spatially constant pairing potential inside the spacer $\Delta_0 = \Delta_0(L)$ (see section 4.3 for details). The Fermi wave-vector in the spacer is obviously $k_F^{spacer} = \sqrt{\mu - U_0} = 0.894\,k_F$ and the spacer coherence length is in our (E_F, k_F^{-1}) units

$$\xi_0 = \frac{2}{\pi\Delta_0}\sqrt{\mu - U_0}. \tag{36}$$

4.1. Interface–interface force

The interface–interface contribution to the total grand potential of our system can be identified from the decomposition

$$\Omega_{tot} = \Omega_{bulk} + 2\Omega_{interf} + \Omega_{i-i} \tag{37}$$

where Ω_{bulk} is the *pro rata*, homogeneous bulk contribution, Ω_{interf} is a surface tension contribution and the remaining part—Ω_{i-i}—can be ascribed to the interaction of the two interfaces (Bruno and Györffy 1993). If our model (see figures 1 and 2) is to be a realistic one, we have to allow the constant pairing potential Δ_0 inside the spacer to depend on its thickness L, $\Delta_0 = \Delta_0(L)$ (cf. studies of Kobes and Whitehead (1987) or of Radović *et al* (1988) and references therein). That means that, generally, the single-interface grand potential Ω_{interf} depends on L (as $\Omega_{interf} = \Omega_{interf}(\Delta_0) = \Omega_{interf}[\Delta_0(L)]$) and so does the grand potential of the homogeneous spacer per unit volume, $\omega_{spacer} = \omega_{spacer}(\Delta_0) = \omega_{spacer}[\Delta_0(L)]$.

The bulk contribution can be decomposed into the spacer and host parts,

$$\frac{1}{A}\Omega_{bulk} = \omega_{host}\,(d - L) + \omega_{spacer}(L)\,L \tag{38}$$

where A is the area of the interface and ω_{host} is the (L-independent) grand potential density of a homogeneous host. By differentiating (37) we get

$$\begin{aligned} f^{tot}(L) &\equiv \frac{1}{A}\,\frac{\partial\Omega_{tot}}{\partial L} \\ &= [\omega_{spacer}(L) - \omega_{host}] + L\frac{\partial\omega_{spacer}(L)}{\partial L} + 2\frac{\partial\Omega_{surf}(L)}{\partial L} + \frac{1}{A}\,\frac{\partial\Omega_{i-i}(L)}{\partial L}. \end{aligned} \tag{39}$$

Another expression ('force formula') for $f^{tot}(L)$ avoiding direct reference to Ω_{interf} or Ω_{i-i} can be derived using standard density functional techniques. The whole procedure is discussed at length in appendix C. Here, we merely quote that in case of symmetrical steplike potentials $U_\alpha(x)$ and $\Delta_0(x)$ (as depicted in figure 2), such an expression acquires the following particularly simple form:

$$\begin{aligned} f^{tot}(L) = (U_{in} - U_{out})\,n\left(\frac{L}{2}\right) + \frac{1}{2}s_{out}\,m\left(\frac{L}{2}\right) - 2\Delta_0(L)\,\chi\left(\frac{L}{2}\right) \\ -2\frac{\partial\Delta_0(L)}{\partial L}\int_{-L/2}^{L/2}\mathrm{d}x\,\chi(x) \end{aligned} \tag{40}$$

where U_{in} and U_{out} are the spin-averaged potential inside the spacer and the host, respectively, s_{out} is the constant exchange splitting in the host, $\Delta_0(L)$ is the spatially constant L-dependent pairing potential inside the spacer and $m(x)$ is the magnetization (see appendix C for more details). Equation (40) is much more suitable for most applications than direct computation of Ω_{tot} from (4) and subsequent numerical differentiation, mainly due to lower CPU time requirements (see beginning of section 4.3 for a detailed discussion).

If Δ_0 does not depend on L, the decomposition (39) reduces to

$$f^{tot}(L) = (\omega_{spacer} - \omega_{host}) + \frac{1}{A}\,\frac{\partial\Omega_{i-i}(L)}{\partial L} \tag{41}$$

which means that the interface–interface force $f_{i-i}(L) \equiv (1/A)\,(\partial\Omega_{i-i}/\partial L)$ can be found from (40) as the L-dependent part of the total force $f^{tot}(L)$ (possibly up to an additive constant). In a normal case ($\Delta_0 = 0$), $f_{i-i}(L)$ acquires the well known oscillatory form

$$f_{i-i}(L) \sim \frac{1}{L^2}\,\sin(2k_F^{spacer}L). \tag{42}$$

Following the results of section 3 and of Bruno and Györffy (1993), we assume that in the case of a superconducting spacer, the interface–interface force $f_{i-i}(L)$ will display oscillations with L of the same frequency. This makes it possible to single out the oscillatory part of $f_{i-i}(L)$ even if Δ_0 is monotonically L dependent: it will be just that part of the total force $f^{tot}(L)$ as obtained by (40) which oscillates with L with the periodicity $2k_F^{spacer}$. In the following investigation, we will always identify $f_{i-i}(L)$ in this way.

4.2. *Magnetic contribution to interface–interface forces*

So far, we have been dealing only with a 'symmetrical' trilayer system, i.e. with a system where the potential inside the host on both sides of the non-magnetic spacer is the same. However, in the case where we are dealing with a non-magnetic spacer and a ferromagnetic host, the magnetic splitting $U_\downarrow - U_\uparrow$ can be in principle of a different sign at each side of the spacer—the magnetic ordering can be either parallel or antiparallel (cf. figure 10), depending on the coupling across the non-magnetic spacer. The oscillatory nature of this magnetic coupling is one of the most striking experimental characteristics of magnetic multilayers (Mathon 1991, Bruno and Györffy 1994).

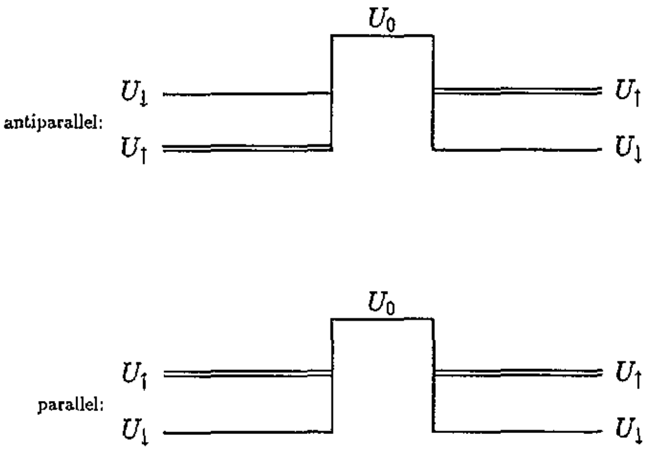

Figure 10. Schematic depiction of the antiparallel ordering (upper scheme) and of the parallel ordering (lower scheme) of the magnetic moments in the host metals of a trilayer system.

The natural 'definition' of the magnetic coupling (and also the one which is directly related to measurable quantities) probably is that of Edwards *et al* (1991), viz.

$$\delta\Omega_{mag}(L) = \Omega_{\uparrow\uparrow}(L) - \Omega_{\uparrow\downarrow}(L) \tag{43}$$

where $\Omega_{\uparrow\uparrow}(L)$ is the grand potential for the parallel ordering of the system and $\Omega_{\uparrow\downarrow}(L)$ that for the antiparallel ordering. The coupling force $f_{MC}(L)$ related to (43) could be defined as

$$f_{MC}(L) \equiv \frac{1}{A}\frac{\partial[\delta\Omega_{mag}(L)]}{\partial L}. \tag{44}$$

If the pairing potential Δ_0 is the same for the parallel and for the antiparallel ordering, the homogeneous bulk parts and the surface term are identical for both types of ordering. Hence, the force $f_{MC}(L)$ is determined only by the interface–interface interaction. As it deals with the isolated magnetic part of the total grand potential, it is natural to expect that the force $f_{MC}(L)$ should describe some sort of 'magnetic' contribution to the interface–interface force.

Another way to define the 'magnetic' part of the interface–interface coupling is to consider the force formula, which for the parallel ordering takes the form given in equation (40). Evidently, we can distinguish between the electrostatic $f_{\uparrow\uparrow}^{es}$ and the magnetic $f_{\uparrow\uparrow}^{mag}$ contributions to the force and we may define

$$f_{\uparrow\uparrow}^{es}(L) = (U_{in} - U_{out})\, n\left(\frac{L}{2}\right) - 2\Delta_0\left|\chi\left(\frac{L}{2}\right)\right| - 2\frac{\partial\Delta_0}{\partial L}\int \mathrm{d}x\, \chi(x) \tag{45}$$

and

$$f^{mag}_{\uparrow\uparrow}(L) = \frac{1}{2} s_{out}\, m\left(\frac{L}{2}\right) \tag{46}$$

satisfying of course

$$f^{tot}_{\uparrow\uparrow}(L) = f^{es}_{\uparrow\uparrow}(L) + f^{mag}_{\uparrow\uparrow}(L).$$

Correspondingly, the total grand potential Ω_{tot} can be divided into its electrostatic and magnetic parts Ω_{es}, Ω_{mag} by

$$\frac{1}{A}\Omega^{es}_{\uparrow\uparrow}(L) = -\int_L^\infty f^{es}_{\uparrow\uparrow}(L) \tag{47}$$

$$\frac{1}{A}\Omega^{mag}_{\uparrow\uparrow}(L) = -\int_L^\infty f^{mag}_{\uparrow\uparrow}(L) \tag{48}$$

$$\frac{1}{A}\Omega^{tot}_{\uparrow\uparrow}(L) = -\int_L^\infty f^{tot}_{\uparrow\uparrow}(L). \tag{49}$$

Extending naturally the approach of Bruno and Györffy (1993), we make a conjecture that the magnetic coupling force $f_{MC}(L)$ defined by equation (44) is proportional to the magnetic part of the interface–interface force in parallel ordering $f^{mag}_{\uparrow\uparrow}(L)$ defined by equation (46). That is to say

$$f_{MC}(L) \to 2\, f^{mag}_{\uparrow\uparrow}(L) \tag{50}$$

asymptotically as $L \to \infty$. In what follows we use $f^{mag}_{\uparrow\uparrow}(L)$ in our investigation of the effect of superconductivity on the coupling of ferromagnetic hosts across a non-magnetic spacer. In appendix D we present numerical evidence in support of equation (50).

4.3. Numerical investigation of magnetic coupling in one dimension

As was noted at the beginning of section 3, evaluating the double integral (18) is a computationally demanding process due to the high requirements on accuracy. This demand is by an order of magnitude greater for evaluation of Ω_{tot} than for evaluation of $n(L/2)$ or $\chi(L/2)$: In order to calculate the electron density and other quantities at $L/2$, it is necessary to integrate functions oscillating with frequency basically $L/2$ in k space—see (2), (3) and (9). On the other hand, calculating the grand potential (4) involves products of the functions (9) integrated over the x-coordinate through the length of the whole system d, *implying an integration of functions oscillating with frequency* $d/2$. *As* $d \gg L$ *(see figure 1)*, it is evident that a much denser integration grid is required for evaluating the grand potential in equation (4) than for calculating the forces in equations (40) and (46). Consequently, through most of this section we relied on the force formula. Direct evaluation of Ω_{tot} from equation (4) was performed only for selected cases in order to check the accuracy of our results. In those test cases we found a very good agreement between calculating $\partial\Omega_{tot}/\partial L$ by differentiation of Ω_{tot} and by using (40).

To summarize, our aim is to analyse the damping of oscillations of the magnetic part of the interface–interface force f^{mag} employing equation (46). The interface–interface contribution is isolated by subtracting the non-oscillating parts, as suggested at the end of section 4.1. Note that the asymptotic decay form of the grand-canonical potential Ω and of the force $f \equiv \partial\Omega/\partial L$ ought to be the same if we assume that

$$\Omega \sim \frac{1}{L^n}\exp\left(-\frac{L}{D}\right)\sin(2k_F^{spacer}L). \tag{51}$$

It can be verified easily by differentiating (51) with respect to L and keeping the lowest-order in $(1/L)$ terms only.

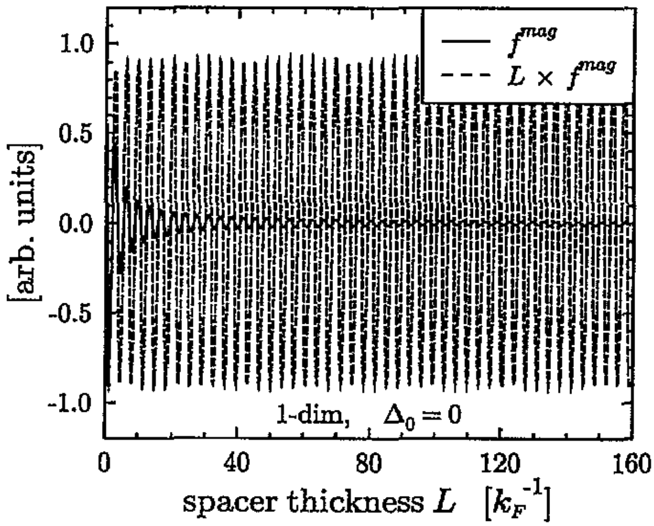

Figure 11. Analysis of the asymptotic behaviour of the magnetic part of the interface–interface force $f_{\uparrow\uparrow}^{mag}$ for a magnetic host and a *non-superconducting* spacer in a proper one-dimensional geometry. The oscillatory part of the magnetic force $f_{\uparrow\uparrow}^{mag}(L)$ together with the $L\, f_{\uparrow\uparrow}^{mag}(L)$ curve are presented.

For a better insight, we analyse the *normal* trilayer system first. It is described by potentials defined in equation (34) and their numerical values presented immediately after equation (35). The well established $(1/L)$ damping of the magnetic coupling, in one dimension, is demonstrated in figure 11, where the oscillatory part of the magnetic force $f_{\uparrow\uparrow}^{mag}(L)$ together with the $Lf_{\uparrow\uparrow}^{mag}(L)$ curve is presented. One can see from the envelope of the $Lf_{\uparrow\uparrow}^{mag}(L)$ oscillations that the 'asymptotic' region begins at $L \sim 10\, k_F^{-1}$, which corresponds (cf. end of section 2.2) roughly to the spacer thickness of five monolayers.

Let us now turn to the same problem for a *superconducting* spacer. The first guess for an asymptote of $f_{\uparrow\uparrow}^{mag}(L)$ might be

$$f_{\uparrow\uparrow}^{mag}(L) \sim \frac{1}{L} \exp\left(-\frac{L}{D}\right) \tag{52}$$

as that would consider both the $\sim 1/L$ decay in a non-superconducting case and the $\sim(1/x)\exp(-x/D)$ decay of Friedel-like oscillations of $\delta n(x)$ (cf. equations (30) and (46)). In what follows we test this the conjecture numerically.

As mentioned in section 4.1, the situation is now conceptually a bit more complicated than it was when studying a single defect (section 3). Namely, the pairing potential Δ_0 is changing as L varies. Clearly, this gives rise to a separate problem of considerable difficulty. This has been studied by a number of authors both theoretically (Werthamer 1963, Radović *et al* 1988, 1991) and experimentally (Banerjee *et al* 1982, Wawro 1993, Strunk *et al* 1994; see also the review of Jin and Ketterson 1989). We deal with it using the approximation of Kobes and Whitehead (1987) and require that our constant $\Delta_0(L)$ is given by

$$\frac{1}{L}\Delta_0(L) = \int_{-L/2}^{L/2} \mathrm{d}x\ (-2\lambda)\ \chi(x) \tag{53}$$

where λ is the usual coupling constant. This approximative gap equation in fact means that we require self-consistency not in $\Delta(x)$ but only in the *integral* of $\Delta(x)$.

As was shown by Kobes and Whitehead (1987, 1988) and by Plehn *et al* (1994), the condition of equation (53) seems to provide a reasonable description of the proximity effect and hence there are good grounds for using it in our calculations as well. In order to check whether a particular choice of the $\Delta_0(L)$ dependence may effect our conclusions significantly, we analyse both the case of L-independent pairing potential ($\Delta_0(L) = \Delta_0\ \forall L$) and the case when $\Delta_0(L)$ conforms to the 'self-consistent constant-gap' condition (53).

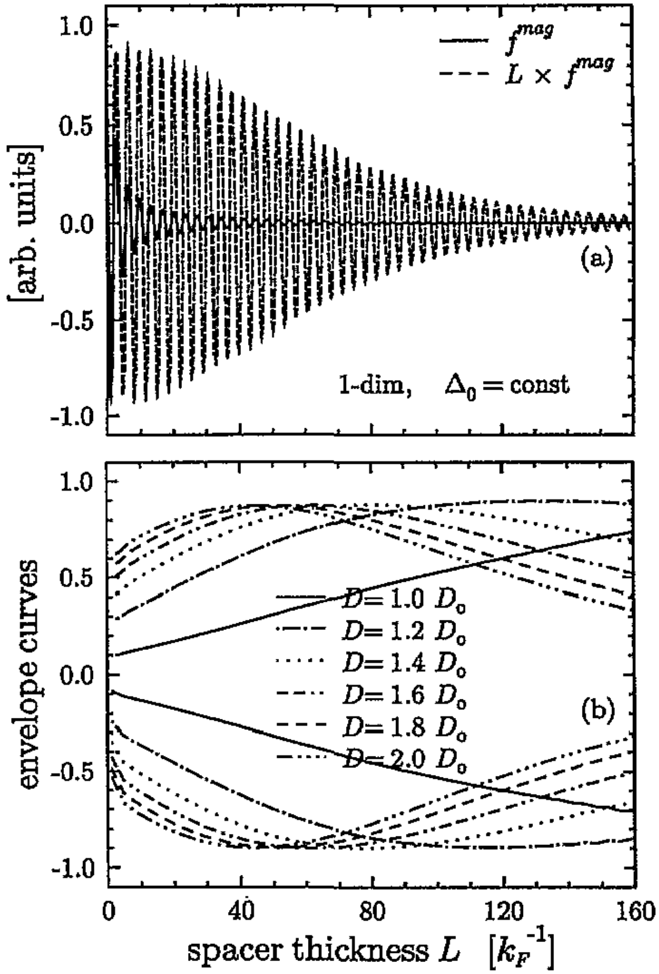

Figure 12. Analysis of the asymptotic behaviour of the magnetic part of the interface–interface force $f_{\uparrow\uparrow}^{mag}$ for a magnetic host and a *superconducting* spacer ($\Delta_0(L)$ = constant) in a proper one-dimensional geometry. In the upper box (*a*), the oscillatory part of the magnetic force $f_{\uparrow\uparrow}^{mag}(L)$ together with the $L\,f_{\uparrow\uparrow}^{mag}(L)$ curve is presented. In the lower box (*b*), the envelopes of $L\exp(L/D)\,f_{\uparrow\uparrow}^{mag}(L)$ curves are presented for several choices of the damping length D.

First, the situation when Δ_0 does not depend on L is analysed. The decay of the oscillatory part of $f_{\uparrow\uparrow}^{mag}$ is studied in figures 12 and 13. Figure 12(*a*) is an analogue to figure 11: it displays the $f_{\uparrow\uparrow}^{mag}(L)$ curve together with $Lf_{\uparrow\uparrow}^{mag}$. It is evident that the

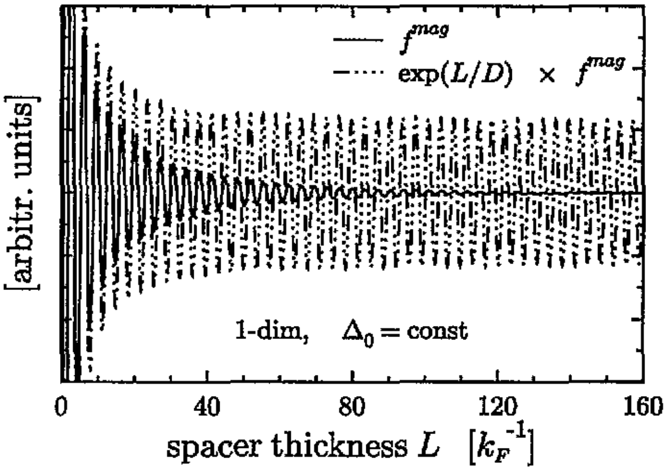

Figure 13. Demonstration of the purely exponential damping of oscillations of the magnetic coupling force $f_{\uparrow\uparrow}^{mag}$ for a magnetic host and a *superconducting* spacer ($\Delta_0(L)$ = constant) in a proper one-dimensional geometry. The exponential damping length is $D = 0.47\,D_0$.

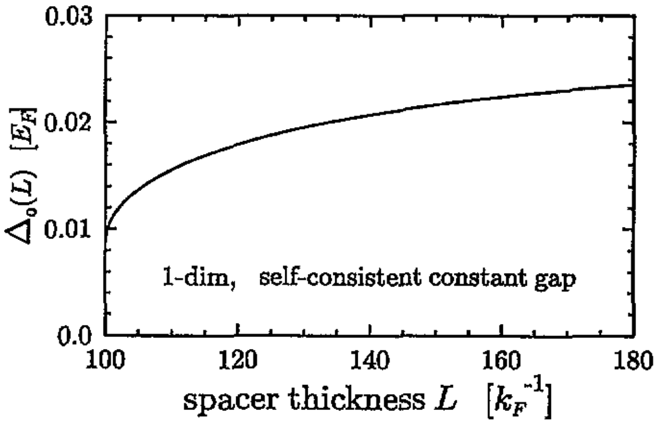

Figure 14. Dependence of the self-consistent constant pairing potential $\Delta_0(L)$ of a superconducting spacer embedded in a magnetic host on the spacer thickness L (proper one-dimensional case).

oscillations now decay faster than in case of a normal spacer. Analysing the damping of $f_{\uparrow\uparrow}^{mag}$ it is found that it is inconsistent with the form (52). To illustrate this, envelopes of $Lf_{\uparrow\uparrow}^{mag}$ curves for several choices of the damping length D are plotted in figure 12(*b*). On the other hand, the decay of the magnetic coupling can be, to a sufficient accuracy, described asymptotically by a *purely exponential* form,

$$f_{\uparrow\uparrow}^{mag}(L) \sim \exp\left(-\frac{L}{D}\right) \qquad (54)$$

as is demonstrated in figure 13 for $D = 0.47\,D_0$. As in sections 3.1 and 3.2, we made the same analysis for other numerical values of the pairing potential Δ_0 as well. We found that the decay form (54) is a general feature of our model. The damping length D does not seem to vary with Δ_0 significantly here, contrary to findings of section 3.

To investigate whether the above trends remain if the pairing potential $\Delta_0(L)$ is allowed to depend on the spacer thickness L, we determined the self-consistent constant pairing potential for the model, described by (35), and present the results in figure 14. The critical thickness L_c (i.e. thickness below which the superconductivity cannot be maintained) is about $\approx 90\,k_F^{-1}$.

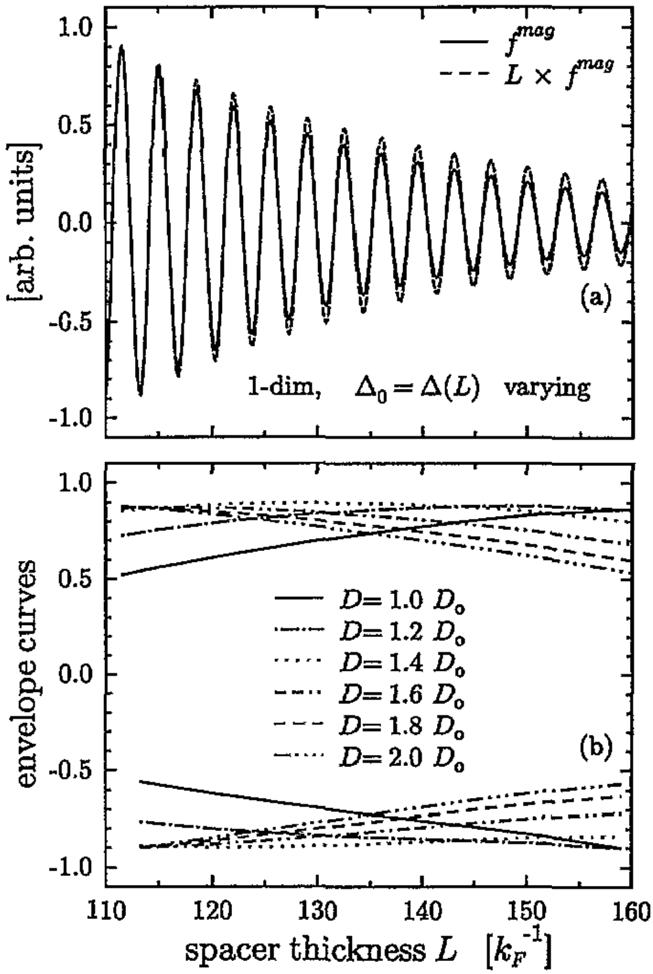

Figure 15. Analysis of the asymptotic behaviour of the magnetic part of the interface–interface force $f_{\uparrow\uparrow}^{mag}$ *for a magnetic host and a superconducting spacer with an L-dependent pairing* potential $\Delta_0(L)$ (proper one-dimensional geometry). In the upper box (a), the oscillatory part of the magnetic force $f_{\uparrow\uparrow}^{mag}(L)$ together with the $L\,f_{\uparrow\uparrow}^{mag}(L)$ curve are presented. In the lower box (b), the envelopes of $L\,\exp(L/D)\,f_{\uparrow\uparrow}^{mag}(L)$ curves are presented for several choices of the damping length D.

The decay formula of equation (52) is tested in figure 15. From the $Lf_{\uparrow\uparrow}^{mag}$ curve presented in figure 15(a) it is clear that the magnetic coupling decays more rapidly than $\sim(1/L)$. Attempts to fit the decay of $f_{\uparrow\uparrow}^{mag}$ to (52) by varying the damping length D are presented in figure 15(b). Similarly to figure 12(b), the agreement is not satisfactory, although the evidence based on figure 15(b) is less compelling as the range of L is considerably smaller. Note that the 'unit' damping length D_0 (and hence also D) depends on L now, because the coherence length ξ_0 does (cf. equations (23) and (36)).

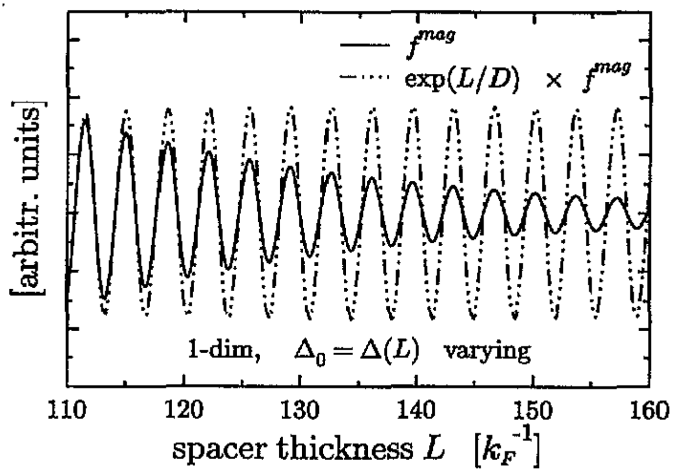

Figure 16. Test of purely exponential damping of the oscillations of magnetic coupling force $f_{\uparrow\uparrow}^{mag}$ for a magnetic host and a *superconducting* spacer with an L-dependent pairing potential $\Delta_0(L)$ (proper one-dimensional geometry). The exponential damping length $D = 0.53\, D_0$ varies with L due to L dependence of ξ_0.

The purely exponential form of the damping is checked in figure 16, where the $f_{\uparrow\uparrow}^{mag}(L)$ curve is presented together with $\exp(L/D) f_{\uparrow\uparrow}^{mag}(L)$ for $D = 0.53\, D_0$. It can be seen that (54) describes the damping of $f_{\uparrow\uparrow}^{mag}(L)$ approximately but as expected the agreement does not seem to be as good as in figure 13. Nevertheless, it is safe to say that including some sort of self-consistency into our model does not essentially alter the general trends observed for fixed Δ_0, although minor changes in the form of the decay of the coupling may occur.

The main result of this section therefore is that the suppression of the interlayer magnetic coupling in a one-dimensional system by superconductivity takes the purely exponential form given in equation (54), instead of the intuitively expected power law modified by an exponential function (52). Unfortunately, to perform the same analysis for a more realistic three-dimensional system using the same procedure as applied here would require too large numerical calculations to contemplate at this stage. Nevertheless, given the results of this section and of section 3, we can assume that, in three dimensions, the decay ought to contain an exponentially decreasing factor. However, the unexpected result of a purely exponential decay in one dimension makes it difficult to guess the answer in three dimensions.

The fact that the oscillatory interface–interface interaction is exponentially damped when the particle–hole distinction is blurred by superconductivity indicates that indeed this interaction is essentially connected with the existence of a Fermi surface. On the other hand, the unexpected form of the cut-off (54) suggests that our understanding of the origin of the magnetic coupling within the RKKY framework may not be complete.

5. Conditions for the experimental observation of the exponential damping

So far we have demonstrated that, for a sandwich trilayer system consisting of a superconductor embedded in a ferromagnetic host, the magnetic oscillatory coupling would be exponentially suppressed when the temperature is lowered below the superconducting transition temperature T_c^S. The question however remains of whether such a suppression would be experimentally observable.

The main obstacle here is the fact that a thin spacer layer of a superconductor remains superconducting only if its thickness L is larger than a certain critical thickness, L_c. This thickness depends both on the spacer (through its coherence length ξ_0, with which we prefer to parametrize the spacer instead of Δ_0 through this section) and on the host (through the exchange energy $s_{out} = U_\uparrow - U_\downarrow$) (Banerjee *et al* 1982, Strunk *et al* 1994). To assess the significance of these factors, we take over the functional form of $L_c = L_c(\xi_0, s_{out})$ from the theory of Radović *et al* (1988). They studied the same model for a superconducting layer embedded in an infinite ferromagnetic host as we have in mind. However, they worked in a dirty limit and used the quasiclassical equations for the Green function integrated over energy and averaged over the Fermi surface (Eilenberger 1968, Usadel 1970)—cf. also Lodder and Koperdraad (1993) for a discussion of various equivalent forms of approximations used in Radović *et al* (1988). In order to transform their results to our clean-limit situation, we substituted in the equations (7), (17) and (18) of their paper for the dirty-limit coherence length ξ_S the BCS coherence length ξ_0 multiplied by 0.541 to account for a different scaling. We arrived at this scaling by comparing the relation for the Ginzburg–Landau coherence length $\xi(T)$ in Radović *et al* (1988) and in Fetter and Hohenberg (1969) and taking the relation between the diffusion coefficient D_S and the mean free path ℓ to be

$$D_S = \tfrac{1}{3} v_F \ell$$

(Deutscher and de Gennes 1969). We also made the diffusion coefficients in the spacer and in the host identical ($D_S = D_M$), and set the boundary condition parameter η equal to one. This last step is motivated by the fact that we require both the wave-functions and their derivatives to be continuous across $x = \pm L/2$ (cf. equation (14) in Radović *et al*'s paper). The purpose of this section is to explore the circumstances where the suppression phenomenon discussed so far becomes experimentally accessible. To facilitate the contact between theory and experiment, all quantities will be measured in 'real life' Rydberg atomic units, Ryd, for energy and au for distances instead of units of E_F and k_F^{-1} as was the case up to now.

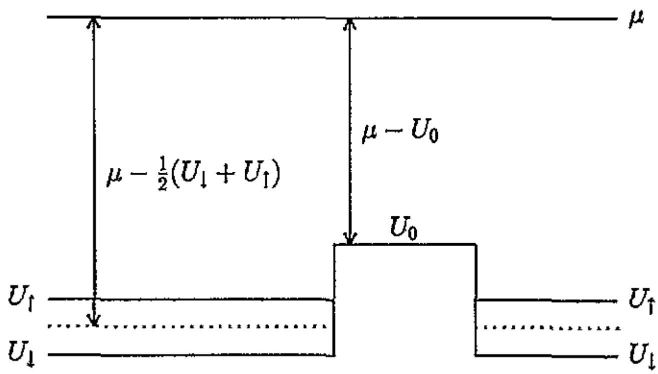

Figure 17. Schematic depiction of the series of systems investigated for the purpose of the exchange splitting s_{out} optimization. The intrinsic characteristics of the spacer as well as of the non-magnetic part of the host, $\mu - U_0$ and $\mu - (U_\uparrow + U_\downarrow)/2$, respectively, are kept constant while the exchange splitting $s_{out} = U_\downarrow - U_\uparrow$ varies. The numerical values used through this section are $\mu - U_0 = 0.60$ Ryd and $\mu - (U_\uparrow + U_\downarrow)/2 = 0.80$ Ryd.

First, we focus on the host and try to find the optimal exchange splitting s_{out}. To do this, we investigate a 'series of systems' such that all characteristics except the exchange splitting s_{out} are constant (figure 17). There are two trends working against each other. One the one hand, larger splitting s_{out} makes the normalized coupling strength J_0 larger (the normalized coupling strength J_0 is defined by Parkin (1991) as the coupling strength for $L_0 = 3$ Å $= 5.67$ au). On the other hand, larger splitting s_{out} means also larger critical thickness L_c, thus decreasing the chance for an observable magnetic coupling at $L \geqslant L_c$. It is hence necessary to assess the combined effect of these two trends.

We calculated the dependence of J_0 on s_{out} for our inhomogeneous jellium model. The coupling strength was calculated from the $\delta\Omega_{mag}(L)$ curve obtained by integration of (48) through the identification $\delta\Omega_{mag}(L) = 2\Omega^{mag}_{\uparrow\uparrow}(L)$ (for details see equation (50) and appendix D) by analysing the oscillation amplitudes for two successive local extrema. The critical thickness L_c as a function of s_{out} can be calculated using the results of Radović *et al* (1988), provided that identifications mentioned at the beginning of this section are made. The dependence of the magnitude of the magnetic coupling when the thickness of the spacer is critical, $J(L_c)$, on the exchange splitting, s_{out}, is then

$$J(L_c) = J_0 \left(\frac{L_0}{L_c}\right)^2 .$$

The results are shown in figure 18 for several choices of the spacer coherence length ξ_0. For comparison, the exchange splitting s_{out} for three ferromagnetic metals is also indicated. It is evident from figure 18 that the magnetic coupling at the critical thickness is a monotonically increasing function of the exchange splitting s_{out} for any choice of the spacer. The reason for this is that the dependence of L_c on s_{out} is rather a weak one for $s_{out} \geqslant 0.01$. In short, superconductivity does not suffer too much from the proximity to magnetic layers for large enough L. Hence, within a clean limit, the suppression of the oscillatory coupling by superconductivity is most likely to be observable for hosts with as large s_{out} as possible.

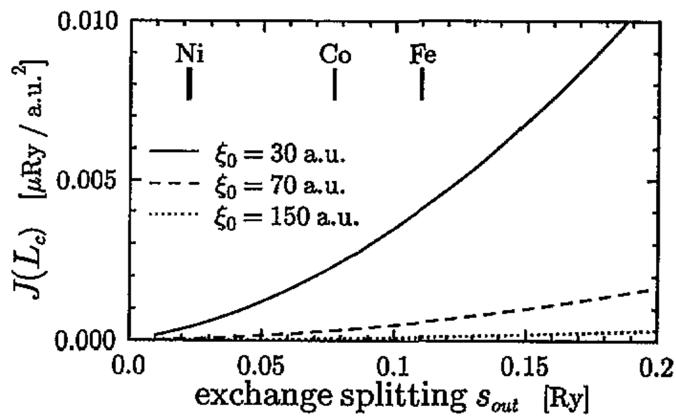

Figure 18. The strength of the magnetic coupling at the critical thickness $J(L_c)$ as a function of the exchange splitting s_{out} for three choices of spacer coherence length. The analogous curve for $\xi_0 = 400$ au would not be distinguishable from the x axis in this scale.

To continue our analysis, we now turn to examining the role of the spacer. Its physical properties can be described within our simple model by the normalized coupling strength J_0 in the normal state and by the BCS coherence length ξ_0. In an ideal case, one should use a material with large J_0 and short ξ_0. However, these two requirements may be in contradiction with one another. Namely, generally, good 'couplers' are expected to be poor superconductors (Parkin 1991). Therefore, it is useful to estimate the magnetic coupling at the critical thickness $J(L_c)$ as a function of both J_0 and ξ_0.

To achieve this, we again make use the results of Radović *et al* (1988) to get the dependence of the critical thickness L_c on the coherence length ξ_0. We found that L_c is nearly directly proportional to ξ_0 and, as noted before, it depends on s_{out} only weakly.

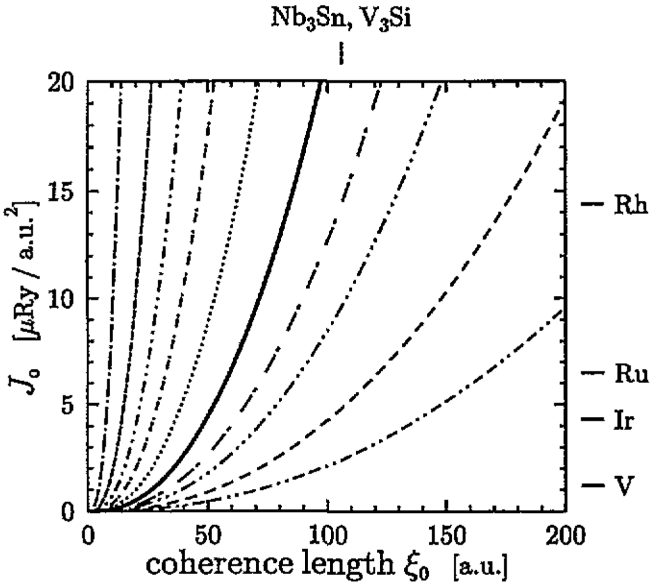

Figure 19. Isolines of constant magnetic coupling strength at the critical thickness of the superconducting spacer $J(L_c)$ as functions of the normalized coupling strength J_0 and the spacer coherence length ξ_0. The host exchange splitting s_{out} is 0.11 Ryd. The individual isolines correspond to $J(L_c) = 0.001$ μRyd au^{-2} (— — · · line), $J(L_c) = 0.002$ μRyd au^{-2} (– – – –), $J(L_c) = 0.004$ μRyd au^{-2} (— · · ·), $J(L_c) = 0.006$ μRyd au^{-2} (— · — ·), $J(L_c) = 0.01$ μRyd au^{-2} (——), $J(L_c) = 0.02$ μRyd au^{-2} (· · ·), $J(L_c) = 0.04$ μRyd au^{-2} (— · — ·), $J(L_c) = 0.08$ μRyd au^{-2} (— · ·), $J(L_c) = 0.20$ μRyd au^{-2} (— — —), $J(L_c) = 1.0$ μRyd au^{-2} (— · —). Bars outside the graph mark the coherence length of A15 compounds Nb_3Sn, V_3Si, and the normalized coupling strengths of transition metals V, Ir, Ru and Rh, respectively. The approximate limit of an experimental resolution (~ 0.01 μRyd au^{-2}) is indicated by a full thick line.

In figure 19, the isolines of a constant magnitude of the magnetic coupling for the critical thickness $J(L_c)$ are presented in the (J_0, ξ_0) plane. We chose the exchange splitting $s_{out} = 0.11$ Ryd, which is the experimental value for an Fe host (Eastman *et al* 1979). Other parameters have the numerical values as presented in figure 17. The thick solid line marks the approximate current limit of the experimental resolution, 0.01 μRyd au^{-2} (Bloemen *et al* 1994, Parkin 1991): if a particular material is represented by a point above that line, the interlayer coupling could still be observable in the normal state for $L = L_c$. The bars outside the plot indicate the experimental BCS coherence length of A15 superconductors Nb_3Sn and V_3Si (Orlando *et al* 1979) and the normalized coupling strengths of selected spacers: $J_0 = 1.2$ μRyd au^{-2} for V, 4.3 μRyd au^{-2} for Ir, 6.5 μRyd au^{-2} for Ru and 14.4 μRyd au^{-2} for Rh (Parkin 1991). It seems to be clear from figure 19 that it is more important to have a short-coherence-length material for the spacer than a material with large normalized coupling strength J_0.

Comparing the indicated parameters of real materials with the position of the thick line representing the limits of experimental resolution, it seems that the coupling would die out before the critical thickness L_c is achieved for most spacers with coherence lengths $\xi_0 \geqslant 10$–

50 lattice spacings. However, given the simplicity of our model, there is a possibility that the real situation is more favourable than figure 19 indicates. Another chance to prepare a suitable system might be to use alloys for spacers, thereby reducing the coherence length ξ_0. Note that, contrary to early views (Blackman and Eliott 1970), disorder should not lead to a decrease in RKKY coupling (de Châtel 1981, Lerner 1991).

In the concluding this section we must comment on the reliability of the above estimates. Evidently, we use a very simple model to describe our trilayer system and the critical thickness L_c was only 'translated' from dirty-limit results of Radović *et al* (1988). Previous studies nevertheless suggest that such an inhomogeneous jellium model yields results which are in order of magnitude agreement with the experiments (Bruno and Györffy 1993). Therefore, we argue that although particular numerical values may be off by factors of order unity, the general trends described in figures 18 and 19 remain.

6. Conclusions

We have investigated a simple inhomogeneous jellium model for a trilayer system with a possibly superconducting spacer on the basis of the Bogoliubov–de Gennes equation. We found that the Friedel oscillations in the electron density $n(x)$ and in the pairing amplitude $\chi(x)$ due to a planar perturbation in the normal U potential are exponentially damped. This conclusion generalizes the earlier result of Fetter for a point defect. However, the particular forms of the damping of Friedel-like oscillations in our model: $\delta n(x) \sim (1/x)\exp(-x/D)$, $\delta\chi(x) \sim \exp(-x/D)$ in one dimension and $\delta n(x) \sim (1/x^2)\exp(-x/D)$, $\delta\chi(x) \sim (1/x)\exp(-x/D)$ in three dimensions are surprisingly different from what might have been expected on the bases of a naive generalization of Fetter's results.

A computational scheme, suitable for investigation of interlayer magnetic coupling across superconducting spacers based on force formulas, was presented. We found that the oscillatory coupling between two ferromagnetic host metals across a non-magnetic spacer is suppressed when the spacer becomes superconducting. Obviously, if observed experimentally, this phenomenon would confirm dramatically that the oscillatory magnetic coupling is closely related to the existence of a well defined Fermi surface. Unexpectedly, in one dimension we did not find a power law prefactor as in $\sim(1/L^n)\exp(-L/D)$. Namely, the pure exponential damping $\sim\exp(-L/D)$ was sufficient to describe our numerical results.

Finally, to facilitate a search for the experimentally most convenient physical systems for which the suppression of the interlayer coupling might be observable, we provided some estimates of the exchange splitting s_{out} and of the spacer coherence length ξ_0 and normalized coupling strength J_0, where the coupling still could be detectable in the normal state.

Acknowledgment

This work was supported by the British SERC (grant G/48381).

Appendix A. Derivation of the BdG equations for a system with a spin-dependent potential

Here, we give a brief derivation of BdG equations (1) presented in section 2.1.

Our arguments will be based on the following Hamiltonian:

$$H_{eff} = \sum_{\alpha} \int d^3r\ \psi_\alpha^+(r)\, H_e(r)\, \psi_\alpha(r) + \sum_{\alpha} \int d^3r\ \psi_\alpha^+(r)\, U_\alpha(r)\, \psi_\alpha(r)$$
$$-\frac{1}{2} \sum_{\alpha\beta} \int d^3r\ \left[\Delta_{\alpha\beta}^+(r)\, \psi_\beta(r)\, \psi_\alpha(r) + \Delta_{\alpha\beta}(r)\, \psi_\beta^+(r)\, \psi_\alpha^+(r)\right] \tag{A1}$$

where

$$H_e(r) = -\nabla^2 - \mu \tag{A2}$$

$U_\alpha(r)$ is a spin-dependent external potential, $\Delta_{\alpha\beta}(r)$ is the pairing potential (considered to be external here), μ is the chemical potential and the usual second quantized notation is used. Rydberg atomic units ($\hbar = 1$, $e^2 = 2$, $m = \frac{1}{2}$) are used in equation (A1) as elsewhere in this paper; the summation $\sum_\alpha$ runs over two spin indexes, $\alpha =\uparrow$ and $\alpha =\downarrow$. The 'conjugate' pairing potential $\Delta_{\alpha\beta}^+(r)$ must satisfy

$$\Delta_{\alpha\beta}^+(r) = \Delta_{\beta\alpha}^*(r)$$

and

$$\Delta_{\alpha\beta}(r) = -\Delta_{\beta\alpha}(r)$$

to ensure real values of the total grand potential $\Omega_{tot} = \langle H_{eff} \rangle$, where $\langle\ \rangle$ denotes quantum as well as thermal averaging.

The Hamiltonian H_{eff} is diagonalized by a Bogoliubov–Valentine transformation

$$\psi_\alpha(r) = \sum_n [u_{n\alpha}(r)\, \gamma_{n\alpha} + v_{n\alpha}^*(r)\, \gamma_{n,-\alpha}^+]$$

provided that the quasiparticle amplitudes $u_{n\alpha}(r)$, $v_{n\alpha}(r)$ satisfy for both $\alpha =\uparrow$ and $\alpha =\downarrow$ the BdG equations (1) presented in section 2.1.

The ground state electron density $n_\alpha(r) = \langle \psi_\alpha^+(r)\psi_\alpha(r)\rangle$, the pairing amplitude $\chi(r) \equiv \chi_{\alpha\beta}(r) = \langle \psi_\alpha(r)\psi_\beta(r)\rangle$ and the total grand potential Ω_{tot} are given by equations (2)–(4). Note that as our Hamiltonian (A1) contains an external pairing potential only, no self-consistency condition occurs in our model. The fully self-consistent theory need not concern us here.

Appendix B. Introducing the cut-off in calculations of the pairing amplitude and of the total grand potential

In order to get finite values of the grand potential Ω_{tot} and of the paring amplitude $\chi(r)$, it is necessary to introduce explicitly an (energy) cut-off in the integrals (2)–(4). This can be demonstrated for the simple case of a uniform superconductor. Provided that $U_0 = 0$ and $\Delta(r) = \Delta_0$, the quasiparticle amplitudes can be written as (de Gennes 1966)

$$u_k(r) = \frac{1}{(\sqrt{2\pi})^3} \sqrt{\frac{1}{2}\left(1 + \frac{k^2 - \mu}{E_k}\right)}\, e^{ik\cdot r}$$
$$v_k(r) = \frac{1}{(\sqrt{2\pi})^3} \sqrt{\frac{1}{2}\left(1 - \frac{k^2 - \mu}{E_k}\right)}\, e^{ik\cdot r}$$

where E_k is the BCS quasiparticle energy

$$E_k = \sqrt{(k^2 - \mu)^2 + \Delta_0^2}.$$

Equations (3) and (4) then lead to

$$\chi(r) = \int_0^{k_{C_2}} \mathrm{d}k \, \frac{1}{4\pi^2} \, k^2 \frac{\Delta_0}{E_k} \tag{B1}$$

and to

$$\frac{\Omega}{V} = \int_0^{k_{C_1}} \mathrm{d}k \, \frac{1}{2\pi^2} \, k^2 \, [(k^2 - \mu) - E_k] + \int_0^{k_{C_2}} \mathrm{d}k \, \frac{\Delta_0}{4\pi^2} \, k^2 \, \frac{\Delta_0}{E_k} \tag{B2}$$

(V is the volume of the superconductor). No cut-off of course corresponds to $k_{C_1} = \infty$, $k_{C_2} = \infty$ (and hence also to $E_{C_1} = \infty$ and $E_{C_2} = \infty$).

As $k \to \infty$, the leading term in the first integrand of (B2) is $-\Delta_0^2/(4\pi^2)$; the leading term in the second integrand of (B2) is $+\Delta_0^2/(4\pi^2)$. The second term in both cases is of order $\sim 1/k^2$. That means that in order to get finite Ω/V in (B2), either both k_{C_1} and k_{C_2} have to be finite or both of them have to be infinite, so that the diverging parts would cancel each other through the whole integration region. However, k_{C_2} cannot be infinite as that would cause $\chi(r)$ to diverge (the integrand in equation (B1) goes like $\sim \Delta_0/(4\pi^2)$ as $k_{C_2} \to \infty$). That means that an explicit cut-off both in (B2) and in (B1) has to be introduced.

This incompleteness of the jellium model seems to be a consequence of our not dealing with the $U(r)$ potential properly—if $U(r)$ is included in the self-consistency procedure, the $\chi(r)$ generating integral of the type of equation (B1) converges naturally without the need for an explicit cut-off (Suvasini and Györffy 1992).

Appendix C. Derivation of the force formula from the density functional theory

In this appendix, we derive the 'force formula' given in equation (40) employing the formalism of the density functional theory for superconductors (Dreizler and Gross 1990).

Our aim is to evaluate the derivative of the total grand potential Ω_{tot} (cf. equations (A1) and (2)–(3)),

$$\Omega_{tot} = \langle H_e \rangle + \sum_\alpha \int \mathrm{d}^3r \, U_\alpha(r) n_\alpha(r) - \int \mathrm{d}^3r \, [\Delta^*(r)\chi(r) + \Delta(r)\chi^*(r)] \tag{C1}$$

with respect to L. Following the arguments of Kohn *et al* (1989) one finds that

$$\Omega_{tot} = F[n, \chi] + \sum_\alpha \int \mathrm{d}^3r \, U_\alpha(r) n_\alpha(r) - 2 \int \mathrm{d}^3r \, \Delta(r)\chi(r) \tag{C2}$$

where $F[n, \chi]$ is a universal functional independent of $U_\alpha(r)$, $\Delta(r)$. Moreover it can be shown that the thermal equilibrium value of Ω_{tot} is the minimum of Ω_{tot} with respect to variations both in $n(r)$ and in $\chi(r)$ defined by equations (2) and (3).

Having this in mind, we can formally differentiate (C2) to get

$$\frac{\partial \Omega_{tot}}{\partial L} = \sum_\alpha \int \mathrm{d}^3r \, n_\alpha(r) \frac{\partial U_\alpha(r)}{\partial L} + \int \mathrm{d}^3r \, [-2\chi(r)] \frac{\partial \Delta(r)}{\partial L}. \tag{C3}$$

To allow for a formal separation of the electrostatic and the magnetic contributions, we express the two components of $U_\alpha(r)$ in terms of a 'spin-averaged' potential $v_a(r)$ and a spin splitting $s(r)$ as

$$U_\uparrow(r) = v_a(r) - \tfrac{1}{2}s(r) \tag{C4}$$

$$U_\downarrow(r) = v_a(r) + \tfrac{1}{2}s(r). \tag{C5}$$

Substituting from (C4) and (C5) into (C3), we can write the force formula for a trilayer system with a superconducting spacer generally as

$$f^{tot}(L) \equiv \frac{1}{A}\frac{\partial \Omega_{tot}}{\partial L} = \int \mathrm{d}x\, n(x)\frac{\partial v_a(x)}{\partial L} - \frac{1}{2}\int \mathrm{d}x\, m(x)\frac{\partial s(x)}{\partial L} - 2\int \mathrm{d}x\, \chi(x)\frac{\partial \Delta(x)}{\partial L}. \tag{C6}$$

The electron density $n(x)$ is as usual given by $n(x) = n_\uparrow(x) + n_\downarrow(x)$ and the magnetization $m(x)$ is defined as $m(x) = n_\uparrow(x) - n_\downarrow(x)$. This is then the principal result of this appendix. Note that the formula (C6) is in its form identical to that derived in Bruno and Györffy (1993) except for the last term which occurs only in the case of a superconducting spacer.

For a 'piece-wise constant' potential,

$$v_a(x) = U_{out}\,\Theta\left(-\frac{L}{2} - x\right) + U_{in}\,\Theta\left(\frac{L}{2} - x\right)\Theta\left(\frac{L}{2} + x\right) + U_{out}\,\Theta\left(-\frac{L}{2} + x\right)$$

$$s(x) = s^{(-)}\,\Theta\left(-\frac{L}{2} - x\right) + s^{(+)}\,\Theta\left(-\frac{L}{2} + x\right)$$

$$\Delta(x) = \Delta_0(L)\,\Theta\left(\frac{L}{2} - x\right)\Theta\left(\frac{L}{2} + x\right)$$

the force formula (C6) can be reduced to

$$\begin{aligned} f^{tot}(L) = {} & \frac{1}{2}(U_{in} - U_{out})n\left(-\frac{L}{2}\right) + \frac{1}{4}s^{(-)}m\left(-\frac{L}{2}\right) - \Delta_0(L)\,\chi\left(-\frac{L}{2}\right) \\ & + \frac{1}{2}(U_{in} - U_{out})n\left(\frac{L}{2}\right) + \frac{1}{4}s^{(+)}m\left(\frac{L}{2}\right) - \Delta_0(L)\chi\left(\frac{L}{2}\right) \\ & - 2\frac{\partial \Delta}{\partial L}\int_{-L/2}^{L/2} \mathrm{d}x\, \chi(x). \end{aligned} \tag{C7}$$

For a symmetrical case (parallel ordering), we have $s^{(-)} = s^{(+)} = s_{out}$ and equation (C7) transforms to (40) as presented in section 4.1.

Appendix D. Numerical test of the definition of the magnetic coupling force $f^{mag}_{\uparrow\uparrow}(L)$

In section 4.2 we defined and in section 4.3 we employed the magnetic coupling force $f^{mag}_{\uparrow\uparrow}(L)$ defined by (46) and (50). In this appendix, we report on a numerical test of the formula in equation (50).

In order to do this, we investigated a one-dimensional sandwich system of a superconducting spacer and a magnetic host as specified in (35). We calculated both the force $f^{mag}_{\uparrow\uparrow}(L)$ evaluated according to formula (46) in the parallel configuration and the force $f_{MC}(L)$ obtained by numerical differentiation of the difference $\Omega_{\uparrow\uparrow}(L) - \Omega_{\uparrow\downarrow}(L)$, as suggested by equation (43). We made numerical calculations for a fixed L-independent pairing potential $\Delta_0 = 0.03\,E_F$ in the range from $L = 2\,k_F^{-1}$ to $L = 120\,k_F^{-1}$ and for an L-dependent Δ potential presented in figure 14 in the range from $L = 110\,k_F^{-1}$ to $L = 120\,k_F^{-1}$. In both cases, the results for $f^{mag}_{\uparrow\uparrow}(L)$ and for $f_{MC}(L)$ agreed within the thickness of a line through the whole range of L.

Although this cannot be regarded as a rigorous proof of relation (50), we feel that for our practical purpose this simple example justifies our reliance on (50) throughout section 4.

References

Andreev A F 1964 *Sov. Phys.-JETP* **19** 1228
Ashida M, Aoyama S, Hara J and Nagai K 1989 *Phys. Rev.* B **40** 8673
Banerjee I, Yang Q S, Falco C M and Schuller I K 1982 *Solid State Commun.* **41** 805
Bardeen J, Kümmel R, Jacobs A E and Tewordt L 1969 *Phys. Rev.* **187** 556
Blackman J A and Eliott R J 1970 *J. Phys. C: Solid State Phys.* **3** 2066
Bloemen P J H, Kestren HW van, Swagten H J M and de Jonge W J M 1994 *Phys. Rev.* B **50** 13 505
Bruno E and Györffy B L 1993 *J. Phys.: Condens. Matter* **5** 2109
——1994 *Appl. Surf. Sci.* **75** 320
Bruno P and Chappert C 1991 *Phys. Rev. Lett.* **67** 1602
Butler H 1976 *Phys. Rev.* B **14** 468
Clinton W L 1992 *Phys. Rev.* B **46** 5742
de Châtel P F 1981 *J. Magn. Magn. Mater.* **23** 28
de Gennes P G 1966 *Superconductivity of Metals and Alloys* (New York: Benjamin)
Deutscher G and de Gennes P G 1969 *Superconductivity* ed R D Parks (New York: Dekker) p 1005
Dreizler R M and Gross E K U 1990 *Density Functional Theory* (Berlin: Springer)
Eastman D E, Janak J F, Williams A R, Coleman R V and Wendin G 1979 *J. Appl. Phys.* **50** 7423
Edwards D M, Mathon J, Muniz R B and Phan M S 1991 *Phys. Rev. Lett.* **67** 493
Eilenberger G 1968 *Z. Phys.* **214** 195
Entin-Wohlman O and Bar-Sagi J 1978 *Phys. Rev.* B **18** 3174
Fetter A L 1965 *Phys. Rev.* **140** A1921
Fetter A L and Hohenberg P C 1969 *Superconductivity* ed R D Parks (New York: Dekker) p 817
Hara J, Ashida M and Nagai K 1993 *Phys. Rev.* B **47** 11 263
Heinrich B, Celinsky Z, Cochran J F, Muir W B, Rudd J, Zhong Q M, Arrott A S, Myrtle K and Kirschner J 1990 *Phys. Rev. Lett.* **64** 673
Jin B Y and Ketterson J B 1989 *Adv. Phys.* **38** 189
Kieselmann G 1987 *Phys. Rev.* B **35** 6762
Kobes R L and Whitehead J P 1987 *Phys. Rev.* B **36** 121
——1988 *Phys. Rev.* B **38** 11 268
Kohn W, Gross E K U and Oliveira L N 1989 *J. Physique* **50** 2601
Lerner I V 1991 *Europhys. Lett.* **16** 479
Lodder A and Koperdraad R T W 1993 *Physica* C **212** 81
Mathon J 1991 *Contemp. Phys.* **32** 143
Orlando T P, McNiff E J Jr, Foner S and Beasley M R 1979 *Phys. Rev.* B **19** 4545
Parkin S S P 1991 *Phys. Rev. Lett.* **67** 3598
Parkin S S P, More N and Roche K P 1990 *Phys. Rev. Lett.* **64** 2304
Plehn H, Wacker O-J and Kümmel R 1994 *Phys. Rev.* B **49** 12 140
Radović Z, Dobrosavljević-Grujić L, Buzdin A I and Clem J R 1988 *Phys. Rev.* B **38** 2388
Radović Z, Ledvij M, Dobrosavljević-Grujić L, Buzdin A I and Clem J R 1991 *Phys. Rev.* B **44** 759
Stojković B P and Valls O T 1994 *Phys. Rev.* B **49** 3413
Strunk C, Sürgers C, Paschen U and von Löhneysen H 1994 *Phys. Rev.* B **49** 4053
Suvasini M B and Györffy B L 1992 *Physica* C **195** 109
Tanaka Y and Tsukada M 1989 *Phys. Rev.* B **40** 4482
Tanaka Y, Yamagami K and Tsukada M 1991 *Solid State Commun.* **79** 349
Usadel K D 1970 *Phys. Rev. Lett.* **25** 507
Wawro A 1993 *J. Phys.: Condens. Matter* **5** 8391
Werthamer N R 1963 *Phys. Rev.* **132** 2440
Zaitlin M P 1982 *Phys. Rev.* B **25** 5729
Ziman J M 1964 *Principles of the Theory of Solids* (Cambridge: Cambridge University Press)